This is to certify that the

thesis entitled
EFFECTS OF POLYMERIC AND GLASS MICROBUBBLE CONTAMINATION ON RECOVERED MATERIALS FROM A LIGHT MEDIUM HYDROCYCLONE SEPARATION OF HIGH DENSITY POLYEHTYLENE FROM POLYPROPYLENE

presented by

EDWARD ARAM AKKASHIAN

has been accepted towards fulfillment
of the requirements for

MASTER degree in PACKAGING

Susan E. Selke
Major professor

Date MAY 18, 1994

EFFECTS OF POLYMERIC AND GLASS MICROBUBBLE CONTAMINATION ON RECOVERED MATERIALS FROM A LIGHT MEDIUM HYDROCYCLONE SEPARATION OF HIGH DENSITY POLYETHYLENE FROM POLYPROPYLENE

By

Edward Aram Akkashian

A THESIS

Submitted to
Michigan State University
in partial fulfillment of the requirements
for the degree of

MASTER OF SCIENCE

School of Packaging

1994

ABSTRACT

EFFECTS OF POLYMERIC AND GLASS MICROBUBBLE CONTAMINATION ON RECOVERED MATERIALS FROM A LIGHT MEDIUM HYDROCYCLONE SEPARATION OF HIGH DENSITY POLYETHYLENE FROM POLYPROPYLENE

By

Edward Aram Akkashian

As the amount of plastic recycled continues to increase, more efficient methods must be developed to collect, separate, and reprocess this recyclable material. This study analyzes the effects that a light medium hydrocyclone separation of high-density polyethylene from polypropylene may have on the materials recovered for reprocessing. The light medium proposed consists of an aqueous suspension of hollow glass spheres used in conjunction with hydrocyclone technology. Tensile, flexural, and impact properties were determined for both pure polymers and for each polymer with low contamination levels by the other polymer and by the glass microbubbles. Also determined were the environmental stress-crack resistance (ESCR), densities, and flow rates of the polymers with and without contaminants.

While some properties of each polymer were adversely affected by the contaminants (impact strength and ESCR), the other properties were either unaffected or enhanced by the various levels of contamination.

ACKNOWLEDGMENTS

I would like to express my sincere appreciation to my major professor, Dr. Susan Selke, Ph.D. (School of Packaging), for her assistance and support. I would also like to thank my committee members Dr. Charles Petty, Ph.D. (Department of Chemical Engineering), and Dr. Jack Gaicin, Ph.D. (School of Packaging).

Special thanks is extended to Mike Rich and Brian Rook of the Composite Materials and Structures Center for their instruction and help with all of the equipment used there. Sincere appreciation is also extended to Mark Sanderson at Himont for his extreme generosity with materials and his time in helping to mold the materials. The generosity of 3M and Quantum for their contribution of materials is also very much appreciated.

TABLE OF CONTENTS

Table of Contents (cont'd)

LIST OF TABLES

Table

LIST OF FIGURES

Figure

List of Figures (cont'd)

CHAPTER I

INTRODUCTION

As consumer and legislative pressures build on producers of plastic packaging to incorporate more recycled content in their products, new, more efficient methods of recycling must be developed. Presently, most of the recycling infrastructure relies upon manual sortation of commingled containers either at the curbside or at a local materials recovery facility (MRF). The high cost of this process and the low purity of the reclaimed plastic, however, are making apparent the fact that the most economically viable solutions lie in the separation of plastics through automated processes. With the throughput of recycled material increasing tremendously, economies of scale will soon necessitate automatic separation of plastics in replacement of the labor intensive processes employed at manual sorting facilities. Automatic sortation of plastics may be achieved through three routes - macro, micro, and molecular sortation. Macro sortation relies upon identification and separation of entire packages by various scanning techniques as the packages are passed by on conveyors or are dropped in front of a sensor. Micro sortation relies on fundamental properties of different plastics once they are granulated or otherwise made into small chips. Some of the properties currently exploited for

micro sortation are density, elecrostatic charge, tacking temperature, and behavior upon cryogenic impacting. Molecular sortation separates plastics through the use of different solvents or one solvent at varying temperatures.

In the long run, the most viable solution involves the use of micro sortation of collected plastics. Molecular sortation provides a high purity product but at a relatively high cost (1) and solvent retention by the recovered plastics can be a concern. Also, these solvents have their own environmental impacts and it is sometimes hard to justify using these chemicals in order to "save the environment" from plastic waste. Macro sorting has limitations also. Multi-component packages may be classified by just one component causing high levels of contamination, or the package may be diverted from the system entirely, requiring manual sortation or landfilling. Crushed bottles may also cause difficulties in macro sorting facilities. Perhaps the largest advantage of micro separation over macro separation, however, lies not in the separation process, but in the collection of the recyclable plastic. In the curbside collection programs currently employed, a large economic setback is the low weight:volume ratio of the plastic containers collected. This problem cannot be dealt with if macro separation processes are used. The flex memory of plastics inhibits a high degree of densification and may also complicate the separation process. With micro separation, however, granulation at the

curbside would result in a high degree of densification, allowing collection trucks to go on longer routes before returning to the local MRF. This would result in a large reduction in energy and labor costs. Coupled with the generation of a less contaminated (higher value) post consumer resin (PCR) stream, this translates into an opportunity for great economic advantage over other methods of separation.

In light of the numerous advantages of micro sorting over other sorting processes, many efforts have been focused on new methods of micro sortation. The project of which this study is a part focuses specifically on the micro separation of blow molding grade high-density polyethylene (HDPE) copolymer from injection molding grade polypropylene (PP) homopolymer. HDPE and PP can be separated from most of the other commonly used packaging plastics using conventional hydrocyclone technology. The HDPE and PP (along with low density polyethylene), being less dense than water, go to the over flow, while the other plastics (such as PET, PVC, and PS) go to the underflow. In order to generate a valuable stream of resin from the overflow (in the absence of LDPE), HDPE and PP must then be separated from one another. This is being attempted through the use of a light medium hydrocyclone. The densities of blow molding grade HDPE copolymer and injection molding grade PP homopolymer are approximately 0.95 g/cm^3 and 0.91 g/cm^3 respectively. To achieve a medium of the optimal density

for separation, an aqueous suspension of hollow glass microbubbles is being used.

The HDPE being used in this study is typical of the resin used to produce opaque blow molded bottles for products such as laundry detergents, juices, motor oils, and household chemicals. The PP is typical of some of the injection molded spouts and closures that are affixed to or snapped or screwed onto the HDPE blow molded bottles.

In 1993, 2,518 million pounds of HDPE was blow molded into containers of up to two gallons in America (2). That is over one fourth of the total HDPE produced domestically that same year. Because this is such a large, visible, easily identified and collected portion of all the HDPE produced, it is only logical to tap this valuable source of plastic - reducing natural resource consumption while simultaneously diverting this plastic from costly landfills. Of this 2,518 million pounds of HDPE that is blow molded, 1102 pounds are HDPE homopolymer (the type of resin used in milk bottles)(2). Because of their similar densities (HDPE hompolymer density is approximately 0.96 g/cm^3), HDPE homopolymer and HDPE copolymer would both exit through the underflow in the system proposed here. In 1993, 130 million pounds of the copolymer was recycled while 245 million pounds of the homopolymer was recycled. This results in recycling rates of about 9.2 percent and 22.2 percent, respectively (2). Because in some applications the mixing of these two resins may be unacceptable (especially when

environmental stress-crack resistance is necessary), further study of the separation of HDPE homopolymer from HDPE copolymer is suggested. This problem is not addressed here.

528 million pounds of PP were used domestically to produce closures in 1993. This is equal to 6.2 percent of all the PP produced that year (2). Although, presently, emphasis is not placed on PP reclamation, interest is beginning to rise. In 1993 PP recycling doubled to 10 million pounds from 5 million pounds in 1992 (2). Also, if a relatively pure stream of PP is produced as a by-product of HDPE reclaim (through spouts and caps on HDPE and other bottles), this by-product can be sold to help offset the cost of processing the HDPE. This is analogous to the sale of gold, silver, and platinum to help offset the cost of purifying copper after it is removed from its ore. This process could be applied to the light fraction recovered from the separation of PET from the other constituents of soft drink bottles. The labels and caps on these bottles are PP, whereas the base cups are HDPE. This may soon lose its importance, however, as the trend turns towards self-supportive bottles with a petaloid base to replace the HDPE base cups in soft drink bottles. As a result of this trend away from base cups, the amount of HDPE recovered from PET soft drink bottle recycling has dropped from 45 million pounds in 1992 to 35 million pounds in 1993 (2).

The role that this study plays in the overall project is to determine whether or not the properties of products

fabricated from the reclaim exiting the overflow and underflow are significantly reduced from products formed from pure, uncontaminated resin. Also, increased strength, reduced density, or any other value adding properties discovered will be noted in an attempt to offset the cost of processing a recycled resin stream.

In order to attribute property differences solely to contamination from the hydrocyclone separation employed (and not to reprocessing techniques or other forms of contamination) virgin resins were used in all the tests conducted. Contamination of each polymer by the other was studied in addition to studying contamination by the hollow glass microbubbles in each of the polymer matrices.

CHAPTER II

LITERATURE REVIEW

Because the method of separation proposed here is a unique idea, no empirical research pertaining to the effects that low levels of spherical glass contaminants may have on polymer properties was found. There have, however, been many models proposed to estimate the effects that spherical fillers have on the properties of plastics. There is a subtle, yet important, distinction between these two classifications. When considering fillers, a larger percent loading is usually assumed. At the lower levels typical of contamination, these models may not hold up well, and may even predict a deterioration in polymer properties when an increase is actually observed (3). Also, the models based on spherical fillers do not address the problem of breakage. As we will see later, breakage - in some processes - is a very realistic concern.

Although the effects of spherical inclusions as contaminants in polymers have not been addressed in the literature, PP and HDPE blends have been studied both as a contaminant in each other and also as blends from the viewpoint of enhancing polymer properties. In the latter case, however, most of the studies include a third agent used as a compatibilizer.

2.1 Effects of Glass Bubbles in the Polymer Matrices

2.1.1 Particle Description - In this literature review the microbubble contamination will be referred to as a "filler", as all the prior research done on spherical inclusions in a polymer matrix has assumed their presence to be as such. In addition to the properties of the two components of a filled polymer and the volume fraction of the filler, ϕ, other factors that affect the properties of the composite include the size, shape, and dispersion of the filler and also the degree of adhesion between the filler and the polymer matrix (4). Particle shape and size is often reflected through the maximum packing fraction, ϕ_m, of a filler. For random loose packing of spheres, ϕ_m is approximately 0.60 (3). In this review of the literature spherical inclusions with good dispersion and little or no adhesion to a non-polar crystalline matrix of high elongation will be considered whenever possible. When only more general models are available, these will be examined. In all models the subscript "$_p$" will denote "polymer" and the subscript "$_R$" will denote the ratio of the composite property to the pure polymer property. ϕ will represent volume fraction filler which will vary, while ϕ_m will represent the maximum packing fraction of the filler, which we approximated as 0.60 for random loose packing of spheres.

2.1.2 Tensile Properties - Quantitative models for tensile strength at yield predict a decrease in strength with an increase in volume load of spherical fillers with

little or no adhesion to the matrix. This is because the continuity of the polymer matrix is displaced by what are essentially voids caused by a lack of adhesion. Several proposed models include:

$$\sigma_R = (1 - \phi/\phi_m)A \qquad (3)$$

$$\sigma_R = (1 - 1.21\phi^{2/3}) \qquad (5)$$

where:

σ_R = the relative tensile strength at yield

A = adhesion factor

However, at low volume loadings, fillers may have a very different effect which, at present, cannot be quantified. Specifically, Katz and Milewski stated that non-polar polymers that orient with strain tend to have great improvements with low adhesion particulate fillers (3). Because the filler exerts a viscous drag on the polymer it helps the polymer in molecular orientation, this is seen as an increase in yield strength at concentrations of approximately 0.05 relative filler volume (3).

As with the tensile strength, elongation models predict a decrease in elongation with increased filler volumes. As the long flexible polymer chains capable of slipping past each other are replaced by a rigid filler, lower elongations are expected. In a model presented by Katz and Milewski,

relative elongation of the composite to the pure polymer is predicted by:

$$\varepsilon_R = \left[1 - \left(\frac{\phi}{\phi_m}\right)^{1/3}\right] \qquad (3)$$

This equation has limitations in that it is not specified whether the elongation represents the elongation for tensile strength at yield or the elongation for tensile strength at break. Also, the degree of adhesion between the filler and the matrix is not incorporated into the equation nor is the equation assumed to be used for only good adhesion or only poor adhesion. As noted by Katz and Milewski, however, a high degree of adhesion between the filler and the polymer matrix will result in a greater loss of elongation then with lower levels of adhesion. Also noted is that at low volume loadings fillers may increase elongation at break (increased elongation at yield is rare). This phenomenon is explained by the orientation of the polymer molecules induced by the drag of the filler as explained above (3).

Because an increase in modulus is the most characteristic effect of adding fillers (6), many models have been proposed to predict their effect upon addition to a polymer matrix. Qualitatively, the small inclusions restrict movement and deformation of the polymer molecules. This puts a mechanical restraint on the composite. Bigg (6) presented a variety of models, as follows:

$$E_R = 1 + 2.5\phi$$

$$E_R = 1 + 2.5\phi + 14.1\phi^2$$

$$E_R = \exp\left[\frac{2.5\phi}{1-\phi/\phi_m}\right]$$

$$E_R = \frac{G_f\phi/\left[(7-5\nu)G_p + (8-10\nu)G_f\right] + \phi/[15(1-\nu)]}{G_p\phi/\left[(7-5\nu)G_p + (8-10\nu)G_f\right] + \phi/[15(1-\nu)]}$$

$$E_R = 1 + \frac{9}{8}\left[\frac{(\phi/\phi_m)^{1/3}}{1-(\phi/\phi_m)^{1/3}}\right]$$

$$E_R = \frac{1}{(1-1.25\phi)^2}$$

$$E_R = \frac{1+A\phi}{1-\psi\phi} \qquad \psi = 1 + \left(\frac{1-\phi_m}{\phi_m^2}\right)\phi$$

$$A = f(geometry)$$

where:

E_R = relative modulus

G_f = shear modulus of filler

G_p = shear modulus of polymer

ν = Poisson ratio of polymer

2.1.3 Flexural Properties - No quantitative description of filler effects on flexural strength were found, but in general fillers reduce the flexural strength of a composite as the percent filler increases (3). However, it is also noted that non-polar, rigid polymers with moderate elongations may show an initial increase in flexural strength before a drop occurs at approximately 0.35 relative filler volume (3).

No model was found specifically for flexural modulus but, because of the large overlap in the literature of models for "tensile modulus", "modulus", and "any modulus", it seems that the effects of fillers on flexural modulus of the resulting composite should be similar to the effects on tensile modulus, and the same equations should be representative of this effect.

2.1.4 Impact Strength - No quantitative models exist to correlate the impact strength of a polymer with the inclusion of a filler (6). However, it can be expected that as the volume fraction of a rigid filler is increased, the impact strength of the composite will decrease (3). The rigid inclusions act as stress concentrators and also reduce the continuity of the polymer matrix.

2.1.5 Environmental Stress-Crack Resistance (ESCR) - When in contact with certain chemicals (not solvents of the plastic) and while under stress, some plastics may exhibit failure through cracking when the presence of the stress alone or the chemical alone would not result in failure of

the specimen. Weak areas in the polymer due to amorphous regions, internal stresses, microvoids, or scratches are amplified when a stress is applied (7). This results in a strain in the area of amplified stress causing further reduction of density. The presence of the chemical can swell the amorphous regions and act as a plasticizer, allowing the plastic to deform more. As the plastic deforms its density lowers permitting greater attack by the chemical. The process is self accelerating, eventually resulting in brittle fracture of the polymer (7). Because it is an empirically defined parameter, no model is available to quantitatively relate the ESCR of a composite to the presence of the filler. However, because the presence of microbubbles may create microvoids and built-in stresses (through differences in the coefficient of thermal expansion), it is assumed that the ESCR would decrease with an increase in filler concentration (8). Also, the greater degree of interfacial contact between the polymer and the chemical (through the presence of microvoids) should help accelerate the growth of the crack.

2.1.6 Flow Rate - The flow rate of a polymer is an empirical property that tells the amount of a polymer (in grams per 10 minutes) that is extruded through a capillary at a given temperature and under a given load. If flow rate can be converted to viscosity (a fundamental polymer property), then there are models available to approximate the effect of fillers on the flow rate and viscosity of the

polymer (see Appendix B for the equations used to convert flow rate to viscosity). The properties of importance when considering filler effects on viscosity include filler concentration, size, aspect ratio and shape, stiffness, strength, and interaction between the filler and the polymer matrix (9). However, the models available simplify the situation and reduce the number of variables. Sheldon (9) presents two models to predict the relative viscosity of a polymer filled with spherical inclusions to that of the unfilled polymer:

$$\eta_R = 1 + 2.5\phi$$

$$\eta_R = 1 + 2.5\phi + 14.1\phi^2$$

Aspect ratio and shape for the spherical inclusions are accounted for by the constant 2.5 (Einstein's coefficient, k_E) and relative filler volume is represented by ϕ, but the other variables are not accounted for in these equations. The second equation accounts for particle interaction, while the first equation assumes no such interaction. Using the equation to first obtain the predicted viscosity, flow rate can then be calculated. Another point of importance is the increased wear that fillers may have upon processing equipment.

2.2 Effects of HDPE and PP Cross-Contamination

In addition to the properties of the individual components of a polyblend and the volume fraction of each component, the most significant factors affecting polyblend properties are phase morphology and interphase adhesion (10). Phase morphology deals with the size and shape distribution of the disperse phase as well as the degree of crystallization for both phases. Interphase adhesion is affected by the miscibility of the components present in the blend. HDPE and PP are often considered immiscible when blended together (11). This is seen as definite phase separation between the two polymers. Most often a compatibilizer is added to blends of HDPE and PP to help reduce the size of the disperse phase and increase interphase adhesion or the components are copolymerized creating block or graft copolymers which will have parts of each chain miscible in each polymer. The discussion here will be limited to blends of HDPE and PP with no compatibilizer added or copolymerization intentionally induced. However, during the process of blending, the HDPE and PP may undergo free radical initiation causing grafting of some HDPE and PP molecules. This may be the result of thermal or mechanical degradation.

2.2.1 PP Contamination of HDPE - Because PP tends to reduce the amount of crystallinity in HDPE, physical properties enhanced by crystallinity would be expected to drop with low amounts of PP. The incompatibility of the two

polymers would also be expected to deteriorate the mechanical properties of the HDPE. Several studies of blow molding grade HDPE contaminated with low levels of injection molding grade PP showed that levels of up to 5 weight percent PP in HDPE could be tolerated without significant reduction of properties (12,13). In the study by Christensen, *et al.* (13), ESCR and flow rate were found to increase while density decreased with increasing PP as expected. Most other studies included a compatibilizer as a factor of the study, tested different properties, or used blow molded containers and cannot be compared to the results obtained in this study.

2.2.2 HDPE Contamination of PP - Lovinger and Williams (14) showed that when HDPE is present in PP it may induce a higher degree of crystallinity in the PP. This is because the HDPE nucleates more readily than the PP, causing more sites for the PP spherulites to grow from. This results in a larger number of spherulites with smaller diameters and an increase in overall crystallinity along with an increase in intercrystalline links. This increase in crystallinity results in a maximum observed tensile modulus at a composition of 80 percent PP and 20 percent HDPE (14). Other reports produced similar results at 90 and 75 percent PP (14). For tensile strength and elongation, however, the incompatibility between the polymers seems to dominate over the increased crystallinity resulting in a polymer with inferior properties (14). The deterioration in properties

is much more pronounced for tensile strength and elongation at break than for these same properties at yield. The degree to which each phenomenon (increased crystallinity or incompatibility) will influence different polymer properties may be somewhat dependent upon the degree of strain involved in determining that particular property. Typically, at higher strains incompatibility is dominant reducing the polymer properties, while at low strains increased crystallinity dominates, enhancing the properties of the polyblend (14). HDPE is often added to PP to improve PP's low temperature impact resistance (15,16). However, no studies could be obtained which had empirical data showing the effects that HDPE has on Izod impact strength of PP. The model found to predict the viscosity of dilute polyblends, included, as a variable, the viscosity of the dispersed phase(in this case HDPE). Because the viscosity of HDPE could not be determined the polyblend viscosity could not be predicted (9).

CHAPTER III

MATERIALS AND METHODS

3.1 MATERIALS

3.1.1 Polymer Matrices - Blow molding grade high density polyethylene copolymer in powder form was obtained from Quantum - USI Division. The product code was LX 0100-00 and it is typical of the HDPE used in bottles for detergents, motor oils, household chemicals, some juices, and other consumer products.

Polypropylene was obtained from Himont. This injection molding grade Polypropylene homopolymer was also in powder form (product code 6501), and is typical of the PP used as spouts and closures for HDPE bottles. The small particle sizes of the powdered resins helped to ensure good mixing of the polymer with the fine microbubbles.

3.1.2 Hollow Glass Microbubbles - Scotchlite K20 glass bubbles (product code 70-0704-2956-1) were provided by 3M. These bubbles were composed of 97-100 percent soda lime borosilicate glass and less than 3 percent amorphous silica. The average diameter of these microbubbles (MB) was 31.11 microns with a wall thickness of 1.34 microns and a density of 0.260 g/cm^3.

3.2 METHODS

3.2.1 Method of Sample Preparation - All materials were first dry mixed and then molded into tensile bars on a 75 ton Van Doren Injection Molder. Screw length and diameter were 28 in. and 1.5 in. respectively, with a screw speed of approximately 200 rpm. Zone 1, zone 2, and nozzle temperatures were set for 410° F and mold temperature was set for 60° F for all materials. Injection time was 13 seconds and hold time was 25 seconds at a pressure of 650 psi.

The eighteen materials molded in this fashion included HDPE and PP each with glass microbubble contamination. The levels of microbubble contamination were 0%, .1%, 1%, 2%, and 5% by weight. Also, mixtures of each polymer in the other at levels of 0%, .5%, 1%, 2%, and 5% by weight were molded into tensile bars. These tensile bars were used as molded for testing tensile properties and further modified for use in all other tests.

3.2.2 Tensile Properties - In order to determine tensile strength at yield, tensile modulus of elasticity, and percent elongation at yield, ASTM D 638-86, "Standard Test Methods for TENSILE PROPERTIES OF PLASTICS", was followed. A United Test System testing machine (Model SFM-20) was used to test tensile bars which were injection molded by Himont to conform to Type I specimens under the ASTM standard. A 1000 pound load cell was used with a

cross-head speed of 0.2 in./min. The gage length used was 2 in. and the grip separation was 4.5 in. The stress-strain curves displayed on the computer screen were used to determine the tensile modulus of elasticity. Because of the manual nature of modulus determination the results may be slightly subjective (two points were manually chosen to define the initial linear portion of the stress-strain curve, the computer then generated the line and calculated the modulus). The tensile strength at yield and percent elongation at yield were calculated through use of the load cell and a laser extensometer.

3.2.3 Flexural Properties - The flexural properties tested were tangent modulus of elasticity and stress at 5 percent strain. ASTM D 790-86, "Standard Test Methods for FLEXURAL PROPERTIES OF UNREINFORCED AND REINFORCED PLASTICS AND ELECTRICAL INSULATING MATERIALS", was followed. The samples tested were bars cut from the tensile bars molded by Himont. These cut tensile bars conformed to the requirements established in ASTM D 790-86 (2.5" x 0.5" x 0.125"). The same UTS testing machine used for tensile testing was set up to perform flexural testing. The support span-to-depth ratio used was 16 to 1 to give a support span of 2 in. A cross-head speed of 0.05 in./min. was used with a 20 pound load cell. The test was automatically terminated at a strain of 5 percent and the strength was recorded. The tangent modulus of elasticity was determined in the same

manner as the tensile modulus and likewise may be somewhat subjective.

3.2.4 Impact Strength - Impact strength was determined by following ASTM D 256-84, "Standard Test Methods for IMPACT RESISTANCE OF PLASTICS AND ELECTRICAL INSULATING MATERIALS". Again samples were cut from the tensile bars molded by Himont. The samples conformed to the standard (2.5" x 0.5" x 0.125"). These cut samples were then notched according to the standard to a depth of 0.1 in. with a TMI Notching Cutter (Model TMI 22-05). A TMI Impact Tester (Model 43-02) was then used with a 5 pound pendulum to determine the impact strength of the samples.

3.2.5 Environmental Stress-Crack Resistance - In order to determine the susceptibility of the samples to failure under conditions of stress in the presence of detergents, ASTM D 1693-70 ,"Standard Test Methods for ENVIRONMENTAL STRESS-CRACKING OF ETHYLENE PLASTICS", was followed. Samples were prepared as follows: Tensile bars injection molded by Himont were used to ensure good distribution of the contaminant in the polymer matrix. These tensile bars were then compression molded using a Carver Laboratory Press (Model M). The samples were placed in a steel frame of inside dimensions 6.6" x 6.6" x 0.075". Sheets of aluminum were placed on either side of the plastic tensile bars and then covered with thicker sheets of steel. This "sandwich" was placed into the press and processed as follows:

HDPE + contaminants:
10 minutes at:
- 25,000 psi
- 150° C

cooled to 55° C without manually adjusting pressure

PP + contaminants:
15 minutes at:
- 30,000 psi
- 190° C

cooled to 65° C without manually adjusting pressure

The sheets of plastic molded from the process described above were left to cool and were cut into rectangular samples within 24 hours of their removal from the mold with a Jarmac circular saw. The samples conformed to condition B from the ASTM standard (1.5" x 0.5" x 0.075"). These samples were nicked to a depth between 0.012 and 0.015 inches using a nicking jig made by Custom Scientific Instruments, Inc. They were then bent, placed in sample holders and immersed in a test tube filled with full-strength Igepal CO-630, a non-ionic detergent. The bending clamp, transfer tool, and specimen holders were also made by CSI, Inc. The stoppered test tubes were then placed in a constant temperature bath at 50° C and checked regularly for failure (every day for PP, every hour for HDPE up to 34 hours, then every four hours up to 50 hours, and finally at 80 hours).

3.2.6 Flow Rate - To help understand the effects that contamination may have on the reprocessing of the materials,

flow rates were determined following the standard, ASTM D 1238-86, "Standard Test Methods for FLOW RATES OF THERMOPLASTICS BY EXTRUSION PLASTOMETER". Tensile bars molded by Himont were cut into small pieces to be charged into the cylinder of the plastometer. Procedure A was used for the HDPE + contaminants because the method indicated that Procedure B should only be used for materials having flow rates greater than 0.5 grams per 10 minutes. Procedure B was used for the PP + contaminants so that the viscosity could be determined, this is not possible with Procedure A. The machine used in both procedures was a Ray Ran Melt Flow Indexer (Model 2 'A').

Procedure A - HDPE + contaminants: After heating the cylinder with the piston and die in place at 190° C for 15 minutes, 3 grams of material were charged into the cylinder and the piston was weighted with a 2.16 kg weight (Condition 190/2.16). At the appropriate time the extrudate was cut and a timer was started. After six minutes the extrudate was cut and, after cooling, it was weighed. The weight was multiplied by 1.67 (10 min/6 min) to determine the flow rate in g/10 min.

Procedure B - PP + contaminants: After heating the cylinder, piston, and die at 230° C for 15 minutes, approximately 7 grams of material were charged into the cylinder and a 2.16 kg weight was placed on top of the piston (Condition 230/2.16). The extrudate was cut just as

the automatic timer was triggered at the appropriate time and position. When the piston traveled 6.35 mm the timer was automatically stopped and the time in seconds it took for the piston to travel 6.35 mm was recorded. The factor from Table 5 (ASTM D 1238-86) was then used to determine flow rate in g/10 min for the samples from the following equation:

$$\text{Flow rate, g/10 min} = F/t$$

where:

F = factor from table 5 (ASTM D 1238-86)
t = time of piston travel for length L, s

And the factor, F, is derived from:

$$F = 427 \times L \times d$$

where:

L = length of calibrated piston travel, cm
d = density of resin at test temperature, g/cm^3
427 = mean of areas of piston and cylinder x 600
(600 = 60 sec/min x 10 min)

3.2.7 Differential Scanning Calorimetry - To determine the heat of fusion of the samples, ASTM D 3417-83, "Standard Test Methods for HEATS OF FUSION AND CRYSTALLIZATION OF POLYMERS BY THERMAL ANALYSIS", was followed. Approximately 12.5 milligrams of each sample was cut from the tensile bars molded by Himont. The samples were cut from the same area in each tensile bar to ensure uniform cooling rates. Also,

visual inspection helped to ensure homogeneity in such a small sample. The tests were performed in a Du Pont Instruments 910 Differential Scanning Calorimeter (Model 910001-908). The cell was purged with nitrogen at 50 mL/min gas flow rate and the specimen (sealed inside an aluminum DSC pan) was placed in the cell along with an empty DSC pan as a known reference sample. The cell was heated from ambient temperature to 180° C for HDPE + contaminants and to 200° C for PP + contaminants at a rate of 10° C/min. A base line was then constructed by connecting the two points at which the melting endotherm deviated from the straight base line. After manually choosing these two points (a slightly subjective task) a TA Instruments Thermal Analyst 2200 System displayed the DSC curve along with the heat of fusion in J/g.

3.2.8 Density - In order to determine the density of each of the samples, ASTM D 792-66, "Standard Test Methods for SPECIFIC GRAVITY AND DENSITY OF PLASTICS BY DISPLACEMENT", was followed. Rectangular samples were cut from the tensile bars molded by Himont. These samples were weighed in air. The samples were then weighed in deionized water along with a wire and sinker used to hold and sink the materials which were lighter than water. Next, the wire and sinker were weighed while immersed in water. Specific gravity was computed as follows:

$$\text{Sp gr } 23/23^{\circ}\text{ C} = a/(a + w - b)$$

where:

a = apparent weight of specimen, without wire or sinker, in air
b = apparent weight of specimen and sinker completely immersed and of the wire partially immersed in water
w = apparent weight of totally immersed sinker and partially immersed wire

And the density of the samples was computed as follows:

$$D^{23C}, \ g/cm^3 = \text{sp gr } 23/23^\circ \text{ C} \times 0.9975$$

3.2.9 Scanning Electron Microscopy - In an attempt to characterize the structure of the polymer and contaminant blends and thus to help explain the results of the physical and mechanical testing, scanning electron micrographs were taken of the fracture surfaces of impact-tested samples of HDPE and PP, including pure samples, material with 5 percent glass microbubble contamination, and material with 5 percent polymeric contamination. Also, micrographs were taken of the glass microbubbles alone to compare surface textures. Samples were coated with approximately 188 Angstroms of gold using a Polaron SEM Coating Machine. Then a Jeol JSM-T330 Scanning Microscope was used to view and photograph the samples.

3.2.10 Data Analysis - In all the graphs of this study the error bars represent the 95 percent confidence intervals for the population means of each treatment. If the lines between two treatments do not overlap, it can be said with

95 percent confidence that they are from populations with different means. Analysis of variance (ANOVA) at a confidence level of 95 percent was also run on each group of data to determine whether differences in means were attributed to variances within the same population or to treatments of individual groups (Appendix C).

The literature value located in the bottom left corner of the graphs, gives typical properties of the uncontaminated polymer (either reported in the literature or given as product specifications). The contamination level is given as weight percent and may be converted to approximate volume fraction through Table 1.

Tables of raw data are contained in Appendix A for a more precise representation of the results shown in graphical form.

CHAPTER IV

RESULTS AND DISCUSSION

4.1 Density

4.1.1 Microbubble Contamination of the Polymer Matrices - A significant increase in density was found for all levels of microbubble contamination in both polymer matrices except for the 0.1 percent contamination levels in both polymers. This increase in density was quite different from what was expected and led to the conclusion that significant breakage of the microbubbles had occurred during the injection molding process. This conclusion was later verified through the use of a scanning electron microscope. Figure 1 shows the calculated density of the resins at 100 percent breakage and at zero percent breakage along with the density actually measured for each resin. Calculations were performed to determine the amount of microbubble breakage in each of the polymer matrices. The glass was assumed to have a density of 2.5 g/cm^3. With this assumption microbubble breakage was found to be an average of 88.7 percent and 92.3 percent for HDPE and PP, respectively. Unfortunately, this may not be typical of what would be seen in a closed loop (bottle to bottle) recycling application. Blow molding operations usually run at pressures up to 150 psi (17), whereas the injection molding processes used in this study had a holding pressure of 650 psi. The product information

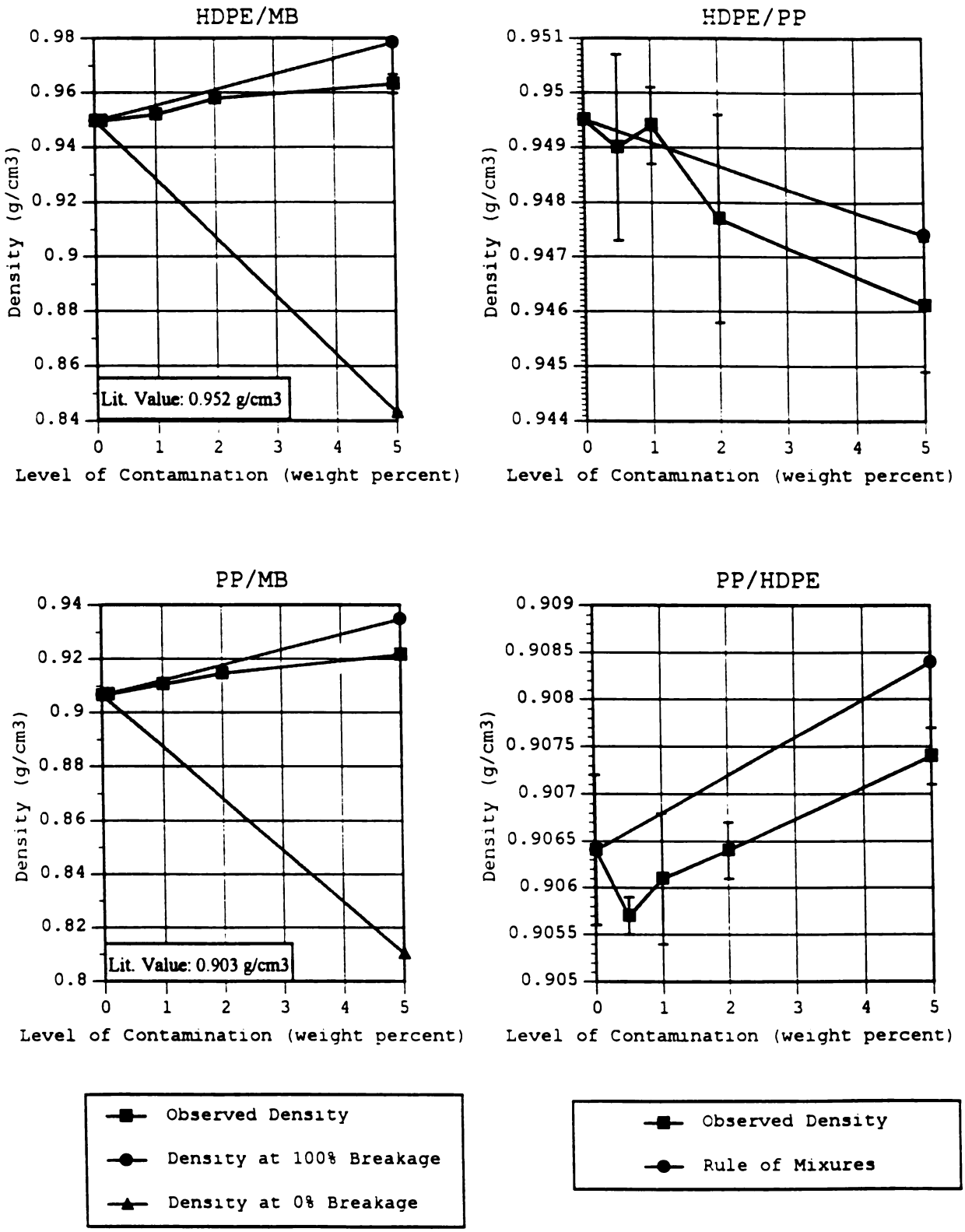

Figure 1: Effects of Contamination on Polymer Density.

pamphlet for the microbubbles indicated that at 500 psi a maximum of 20 percent breakage should occur. Using the averages of 88.7 and 92.3 percent microbubble breakage for HDPE and PP (see Appendix B), the volume fraction of broken and intact glass bubbles was calculated. The total volume fraction of glass (broken plus intact) was used in the model equations for spherical fillers (Table 1). Models for spherical fillers were used because the glass spheres were much easier to characterize than the broken pieces of glass. Also, the volume fraction of glass spheres was very similar to the volume fraction of the broken glass. Spheres comprised approximately 55.1 percent of the glass volume in HDPE and about 44.5 percent in PP (Table 1).

4.1.2 HDPE/PP Cross-Contamination - The only significant change in density from the uncontaminated resins seen for the various HDPE/PP blends was at the 5 percent contamination level of PP in HDPE where a decrease in density was observed (Figure 1). All other blends produced densities within the 95 percent confidence intervals for the uncontaminated resins. However, the trends seen were expected, and the observed densities are plotted against the expected densities based on a simple rule of mixtures in Figure 1. The greater than expected loss in density seen by HDPE may be indicative of a disruption of HDPE crystallinity caused by methyl groups present on the PP chains. The shift of observed density from the expected density in PP may be due to an error in the estimation of the population mean for

Table 1: Characterization of Glass in the Polymer Matrices.

Average of 88.7% Microbubble Breakage for HDPE	Weight Percent Glass 0.1	1	2	5
Density of Contaminated Resin	0.949738	0.95186	0.954186	0.960961
Volume Fraction Broken Bubbles	0.000337	0.003344	0.006638	0.016236
Volume Fratction Intact Bubbles	0.000412	0.004096	0.008131	0.019888
Total Volume Fraction Glass	0.000749	0.00744	0.01477	0.036124

Intact Bubbles Comprise 55.1% of the Glass in HDPE.

Average of 92.3% Microbubble Breakage for PP	Weight Percent Glass 0.1	1	2	5
Density of Contaminated Resin	0.90676	0.909976	0.91351	0.923862
Volume Fraction Broken Bubbles	0.000334	0.003326	0.006613	0.016242
Volume Fratction Intact Bubbles	0.000268	0.002668	0.005305	0.013029
Total Volume Fraction Glass	0.000603	0.005995	0.011918	0.029271

Intact Bubbles Comprise 44.5% of the Glass in PP.

uncontaminated PP. It can be observed from Figure 1 that if the uncontaminated PP had a density of approximately 0.9056 the two lines would coincide very well. The large standard deviation for the pure PP helps to validate this theory.

4.2 Differential Scanning Calorimetry

4.2.1 Microbubble Contamination of the Polymer Matrices - Figure 2 shows the observed heat of melting at various contamination levels plotted against the line for a simple rule of mixtures. As can be seen for both HDPE and PP the heat of melting is below that predicted by a rule of mixtures. This may signify a disruption of the crystalline regions for both the HDPE and the PP.

4.2.2 PP Contamination of HDPE - The trend seen for the HDPE/PP mixture are similar to the trends above (Figure 2). The sharp initial decrease in heat of melting is probably indicative of a disruption in the crystalline structure of HDPE. At higher levels of contamination the heat of melting of the blend begins to approach the weighted average of the two components.

4.2.3 HDPE Contamination of PP - A very different effect was seen with the PP/HDPE blends. Low levels of HDPE actually increased the heat of melting of the PP by more than the weighted average of the two components (Figure 2). This phenomenon may be explained by the high degree of nucleation caused by the presence of HDPE. Once nucleation is initiated by the HDPE the PP spherulites continue to grow at these sites. Without the presence of the HDPE,

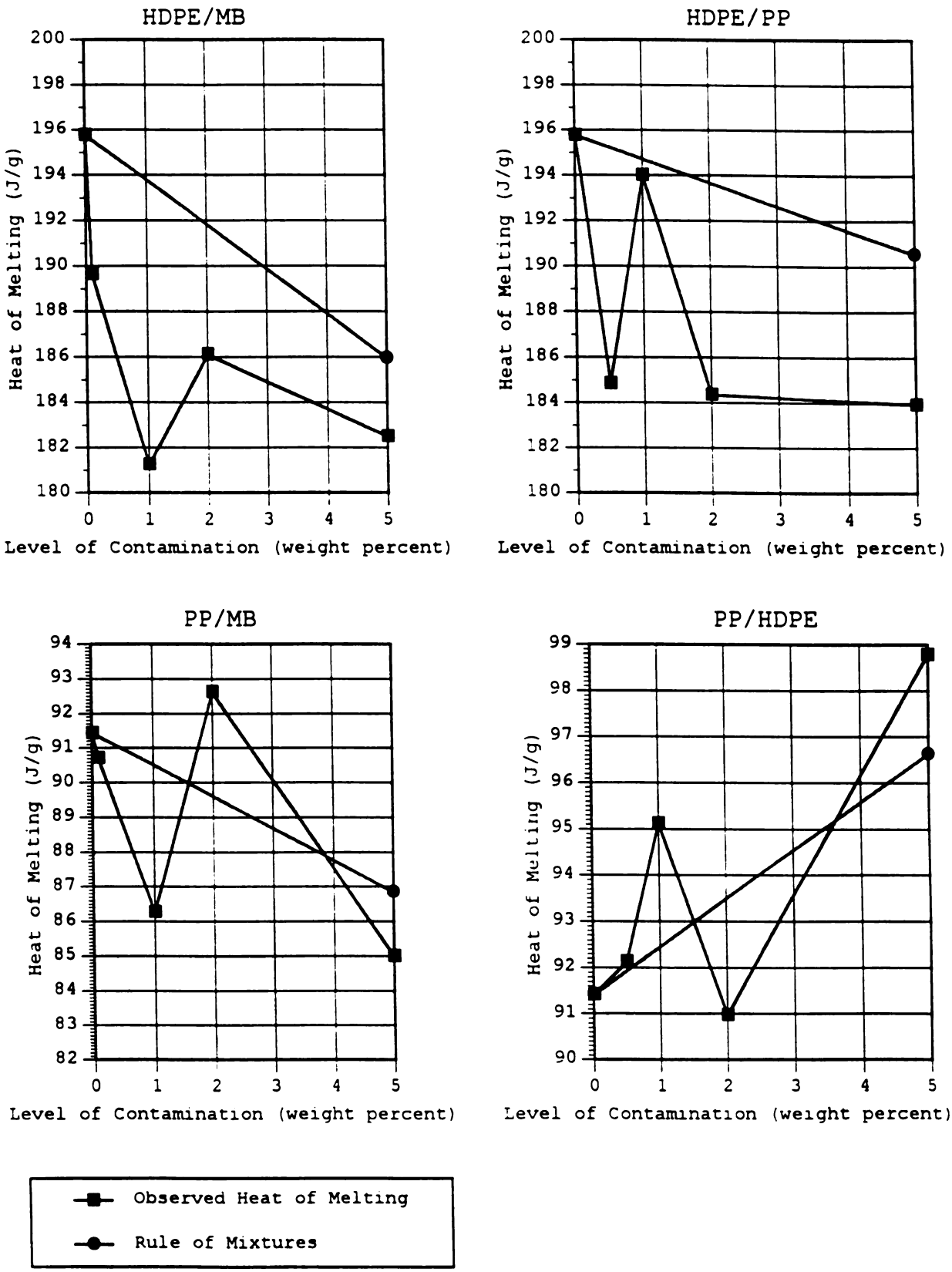

Figure 2: Effect of Contamination on Heat of Melting.

nucleation in PP is much slower resulting in fewer (albeit, larger) spherulites (18).

4.3 Scanning Electron Microscopy

4.3.1 Microbubble Contamination of HDPE - Micrographs of the fracture surfaces of impact tested HDPE with 5 percent microbubble contamination showed good dispersion of the microbubbles in the polymer matrix (Figure 3). Figures 4 and 5 verify that many of the glass bubbles had indeed suffered breakage during processing. Figure 5 shows a typical microbubble/HDPE interface with poor wetting of the glass surface and very little adhesion between the two components. The surface of this glass bubble can be compared to a glass bubble that was not in contact with the polymer (Figure 6). The broken bubbles resulted in many shapes and sizes which made them hard to characterize in model equations.

4.3.2 Microbubble Contamination of PP - Again micrographs of the fracture surfaces were taken and fairly good dispersion of the microbubbles was observed. A higher percentage of breakage seemed quite apparent from the micrographs (Figure 7), which was in accordance with what was calculated from changes in density. Polypropylene seemed to wet the glass surface much better than HDPE, but adhesion was still very minimal (Figure 8). The degree of polymer/glass adhesion and the percent microbubble breakage (through particle shape factors and percent volume loading) are important factors when considering the effects of

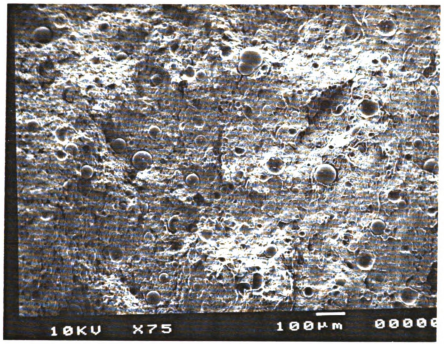

Figure 3: Micrograph of HDPE with 5% Microbubble Contamination.

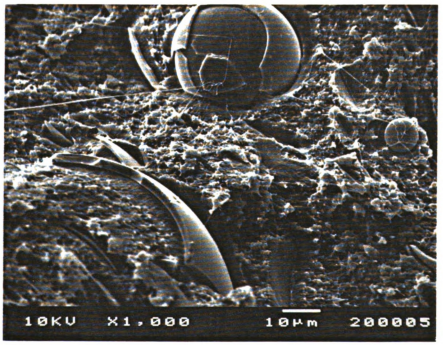

Figure 4: Micrograph Showing Typical Amount of Microbubble Breakage.

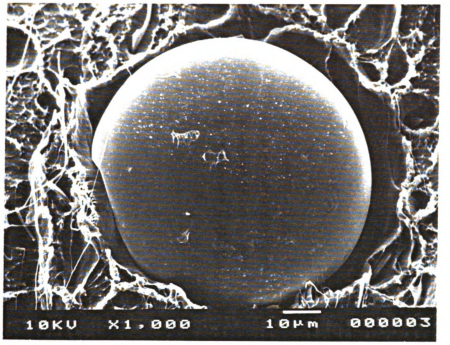

Figure 5: Typical HDPE/Microbubble Interface.

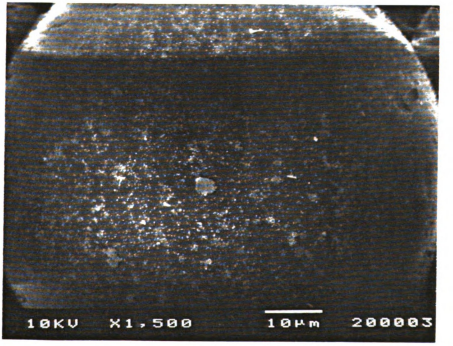

Figure 6: Typical Surface of a Microbubble.

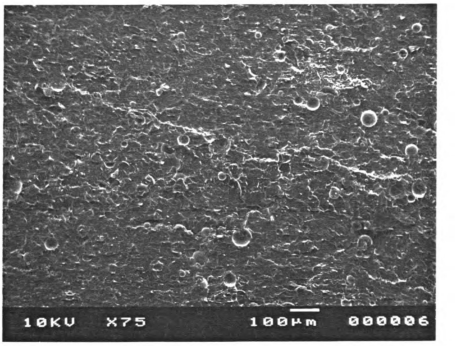

Figure 7: Micrograph of PP with 5% Microbubble Contamination.

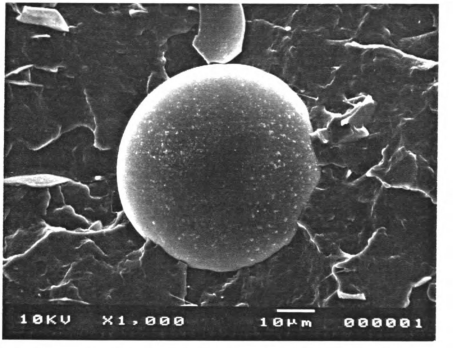

Figure 8: Typical PP/Microbubble Interface.

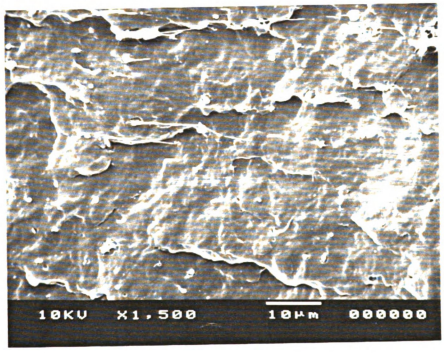

Figure 9: Micrograph of PP with 5% HDPE Contamination.

microbubble contamination on mechanical and physical properties of these polymers.

4.3.3 HDPE/PP Cross-Contamination - SEM study of HDPE with small amounts of PP showed poor dispersion of the PP. Most areas looked similar to the uncontaminated HDPE while other areas contained large agglomerations of PP.

Micrographs of PP with HDPE showed good dispersion, yet definite phase separation of the two polymers (Figure 9). The blend seemed to be anisotropic with elongation of the HDPE occurring in the direction of flow during the injection molding process.

4.4 Tensile Properties

4.4.1 Microbubble Contamination of HDPE - A general increase was seen in tensile strength at yield and in modulus of elasticity, with a sharp increase from the uncontaminated resin to the 0.1 percent level of contamination. After an initial increase at the 0.1 percent contamination level, a decrease was seen in elongation at yield. Figures 10, 11, and 12 show these trends quantitatively and the significance of various levels of contamination can be determined from these graphs. Models studied describing the effects of spherical inclusions with little adhesion to the polymer matrix predicted three trends. An increase in modulus with a decrease in both the tensile strength and elongation. Not represented in the equation by Katz and Milewski (3), however, was a qualitative description of why tensile strength may

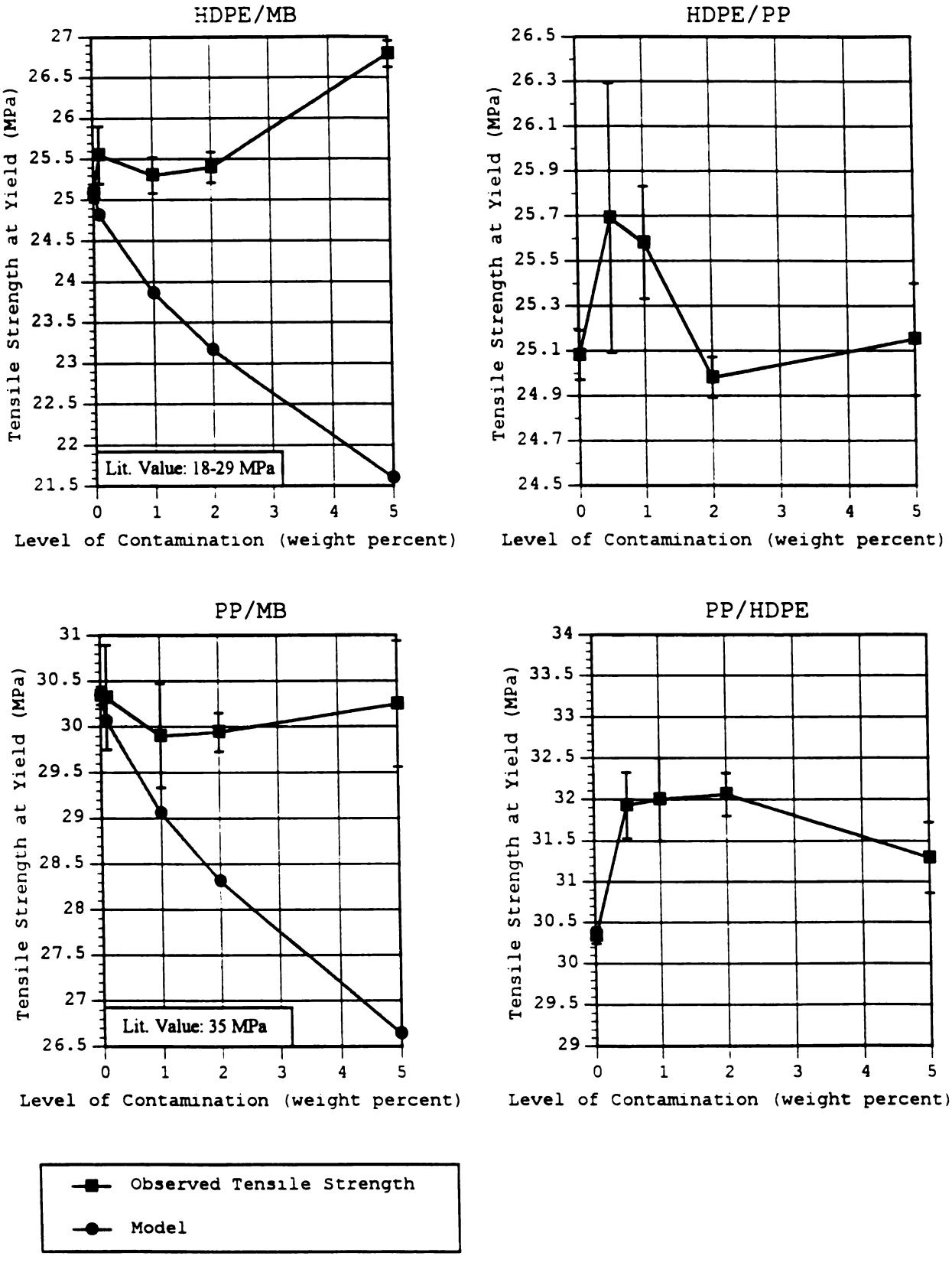

Figure 10: Effects of Contamination on Tensile Strength at yield.

initially increase for filler volumes up to 5 percent (recall, however, that the 5 weight percent filler corresponds to a 0.039 volume fraction of spheres and broken glass in HDPE). This phenomenon is explained by a work hardening effect on the polymer. Because there is little adhesion to the glass, the HDPE may draw around the particles and orient. This is induced by a viscous drag on the polymer by the glass. Work hardening is usually promoted by high aspect ratio fillers because of their greater surface area:volume ratio (3) and the strengthening in this case may be due largely to the broken glass in the matrix.

A higher increase in modulus was observed than predicted and the loss of elongation was not as dramatic as the model had predicted (Figures 12 and 11). Tensile strength experienced an increase which no model could quantitatively predict. All the tensile properties studied for the contaminated resins were higher than predicted by the models. Perhaps this is due to the presence of the broken bubbles (due to their shape), for which no model found could estimate the effects, along with microbubbles, on the polymer matrix. These significant differences, according to Analysis of variance at a confidence level of 95 percent, are attributed to the treatment of groups rather than to variations within the same group.

3.4.2 Microbubble Contamination of PP - Analysis of variance showed no significant changes in tensile strength

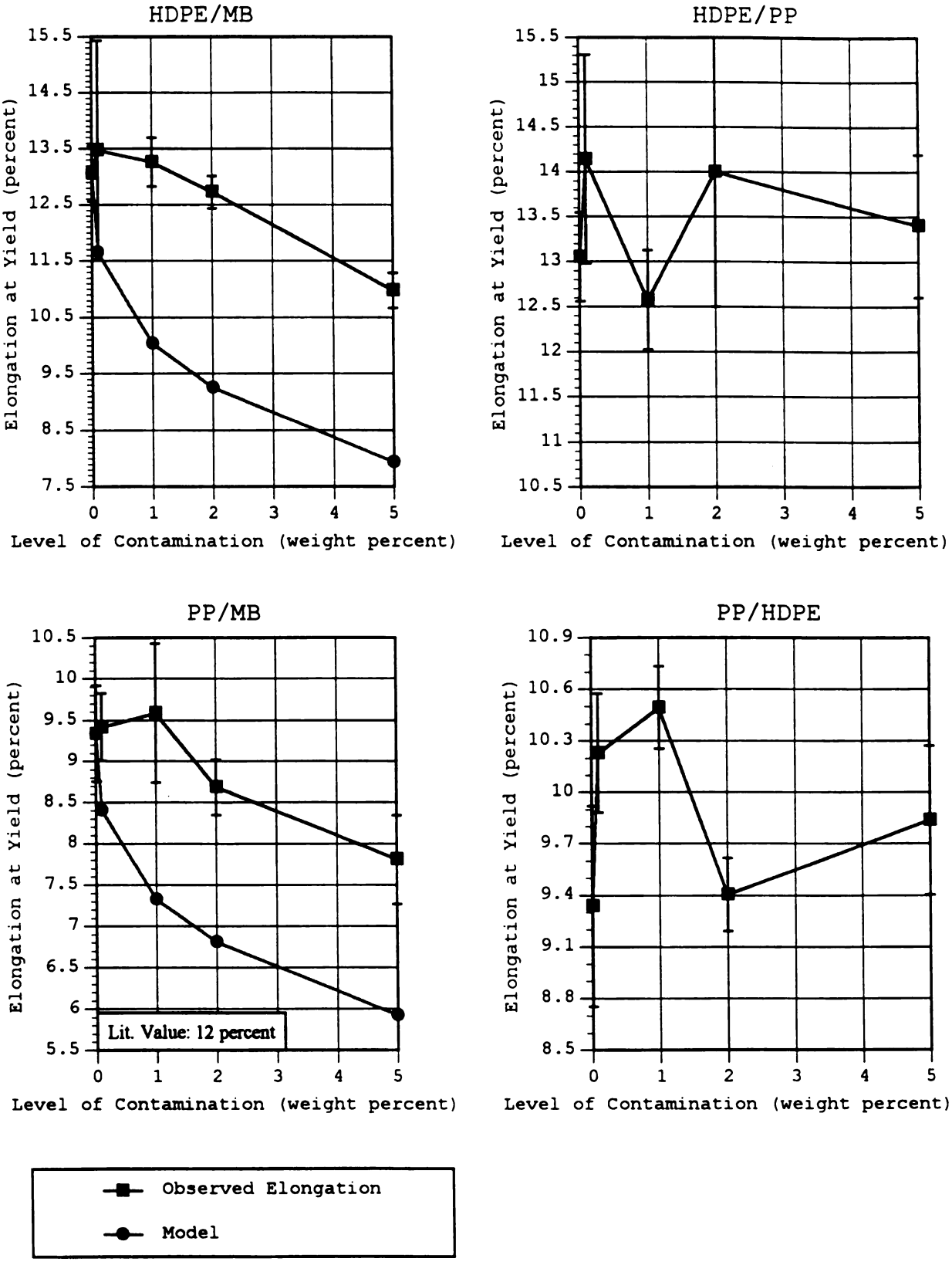

Figure 11: Effect of Contamination on Elongation at yield.

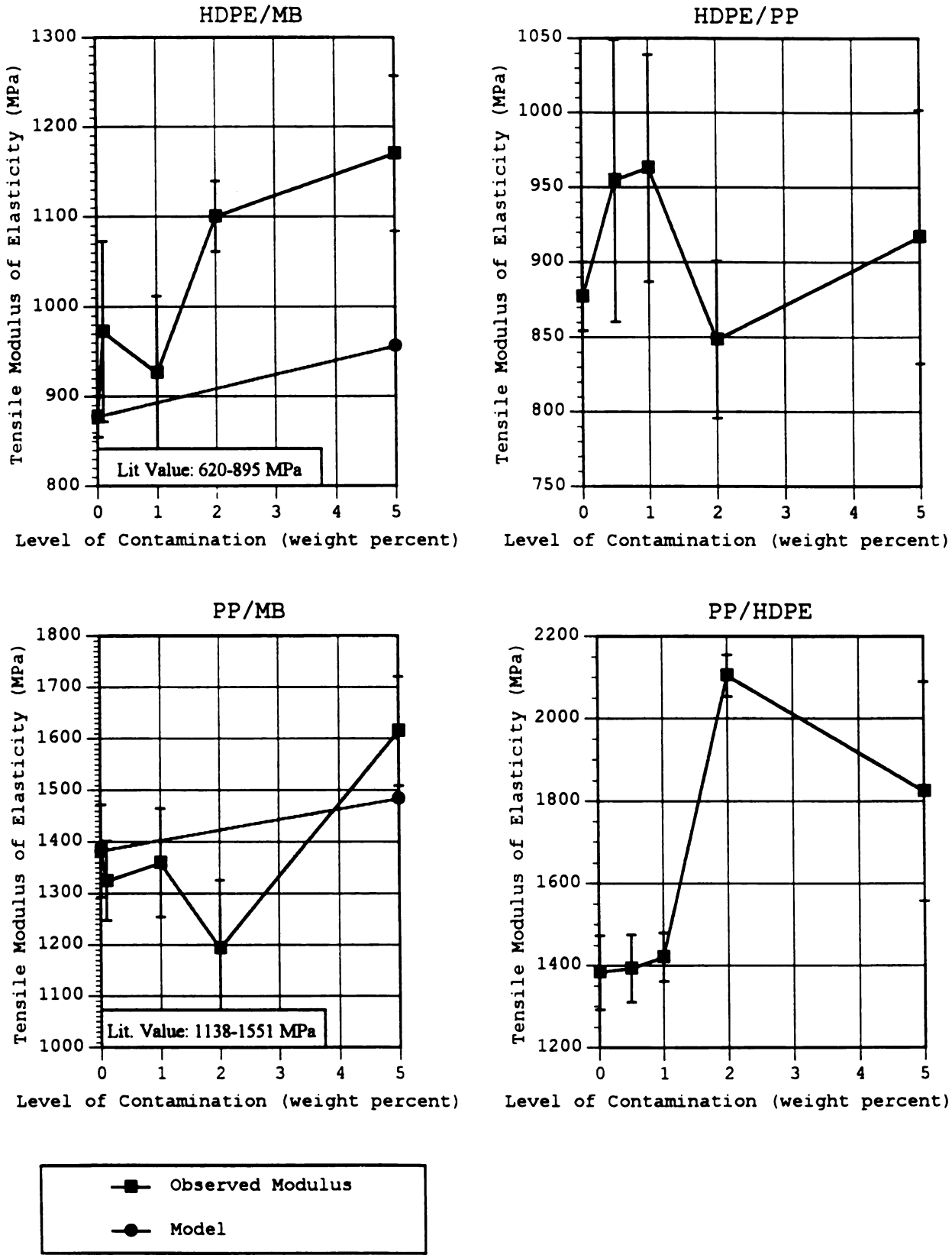

Figure 12: Effects of Contamination on Tensile Modulus of Elasticity.

due to the level of microbubble contamination up to 5 percent. However, variations in elongation and modulus are attributed to the presence of the microbubbles. Elongation is decreased and modulus is increased, which is expected (Figures 11 and 12). The same models were used here as for the effects of microbubble contamination on HDPE.

4.4.3 PP Contamination of HDPE - ANOVA showed no significant change for elongation at yield and tensile modulus. Tensile strength at yield had a quite erratic curve (Figure 10), suggesting, perhaps, that like elongation and modulus, tensile strength of HDPE is also unaffected by low levels of PP contamination.

4.4.4 HDPE Contamination of PP - Tensile Strength at yield and modulus of PP both increased up to 2 percent HDPE contamination and then began to fall (Figures 10 and 12). This initial increase is in accordance with prior research done by Lovinger and Williams (14), Noel and Carley (15), and Deanin and Sansone (16), and is attributed to an increase in the crystallinity of PP as well as an increase in links between the separate spherulites of the PP. However, in these prior works, maxima were observed at 20 percent, 25 percent, and 10 percent, respectively. Elongation at yield increased initially (Figure 11), which was quite unexpected because of the incompatibility of the two polymers.

4.5 Flexural Properties

4.5.1 Microbubble Contamination of HDPE - Both strength at 5 percent strain and the flexural modulus showed a sharp increase from the uncontaminated resin to the resin with 0.001 weight fraction microbubbles. A rather linear increase of lesser slope was seen for higher levels of contamination (Figures 13 and 14). The model predicted well the slope of the line after the initial increase, but could not account for the dramatic initial increase, quantitatively or qualitatively. No quantitative model was found for flexural strength, however, the results can be explained by the viscous drag applied to the molecular chains by the microbubbles on the outer surface where strain occurs (3) and perhaps by an increase in compressive strength at the inner surface where compression occurs. The variations were attributed to the treatment of different groups according to ANOVA, at a 95 percent confidence level.

4.5.2 Microbubble Contamination of PP - Strength at 5 percent strain showed no relation to microbubble inclusion according to ANOVA. Flexural modulus showed an initial decrease followed by a fairly steady increase (Figure 14). The model predicts an increase of flexural modulus, however, the observed modulus increased with a steeper slope.

4.5.3 PP Contamination of HDPE - The flexural properties of HDPE were enhanced by the addition of PP (Figure 12). Because it is well documented that PP disrupts HDPE crystallinity this effect was not expected.

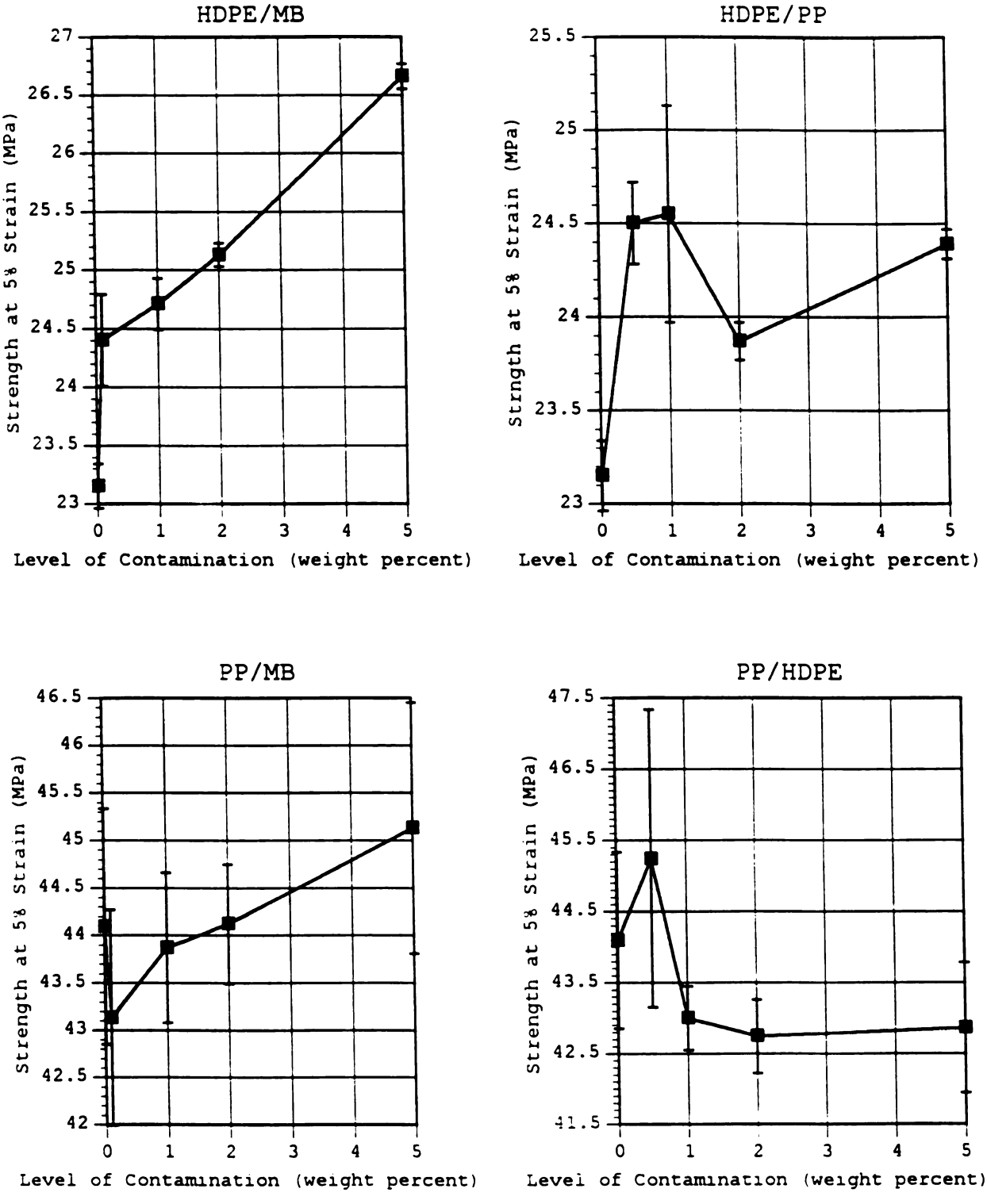

Figure 13: Effects of Contamination on Flexural Strength at 5% Strain.

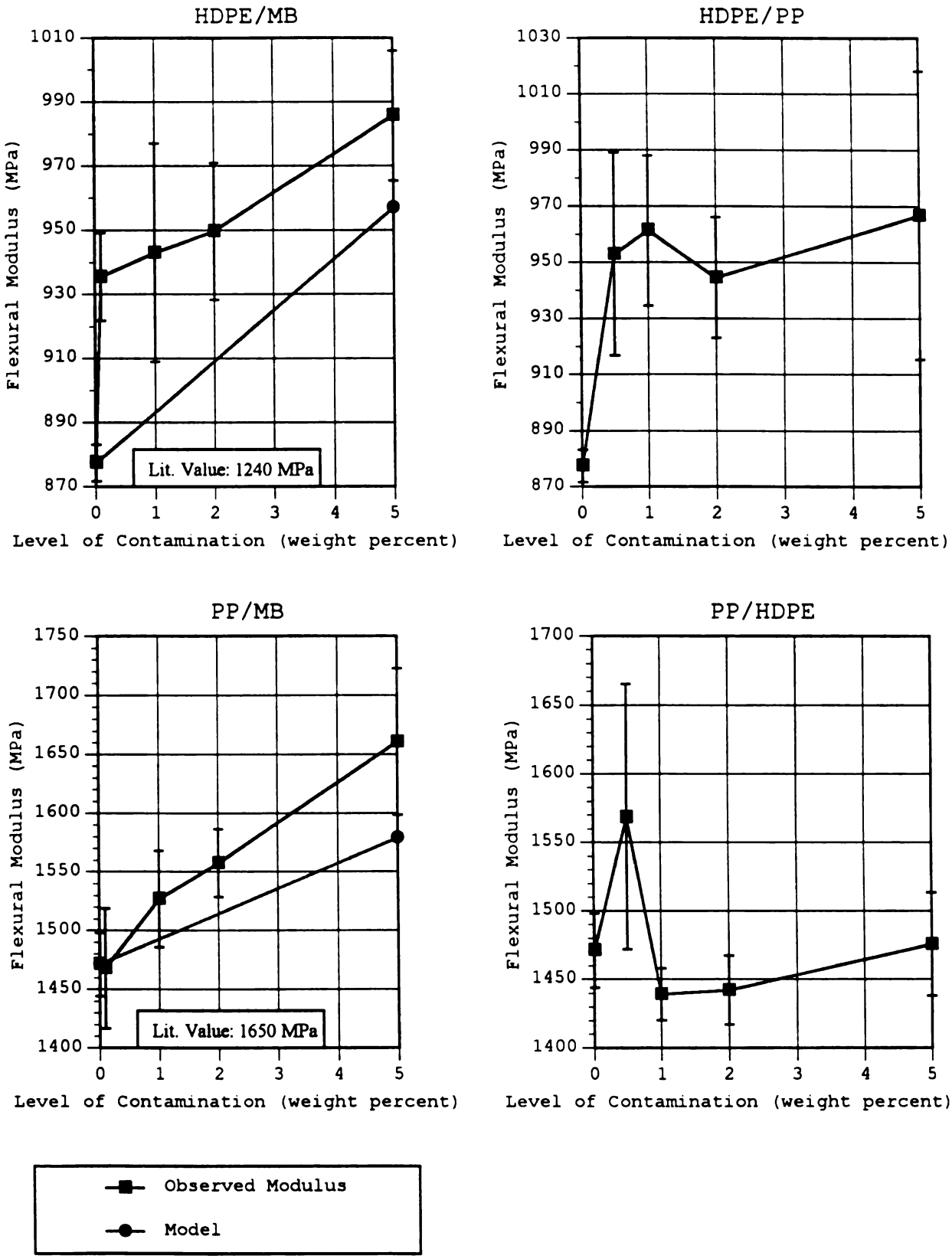

Figure 14: Effects of Contamination on Flexural Modulus of Elasticity.

4.5.4 HDPE Contamination of PP - The flexural properties of PP decreased with the addition of HDPE (Figures 13 and 14). Apparently, the inferior properties of HDPE combined with the incompatibility of HDPE and PP dominated over the increased crystallinity of the PP.

4.6 Impact Strength

4.6.1 Contaminated HDPE - The HDPE samples used for impact testing all resulted in non-breaks with the heaviest weight available (30 pounds). Although the results cannot be quantified, it can be concluded that sufficient embrittlement to cause failure in HDPE did not occur with microbubble or PP contamination.

4.6.2 Microbubble Contamination of PP - A very sharp decrease in impact strength was seen at a microbubble contamination level of 0.1 weight percent and then a slight increase was seen (Figure 15). This sharp initial drop seems to be consistent with prior research done by Bigg (6). In the study by Bigg, PP impact strength was shown to decrease sharply with the addition of 0.01 volume fraction filler and then level off toward a flatter slope. Whereas fibers (as used by Bigg) usually tend to distribute the impact stress over a larger area perpendicular to the force of impact (3), this is not the case for spheres. Thus, greater reduction of strength was observed for the glass spheres than was reported by Bigg for fibers.

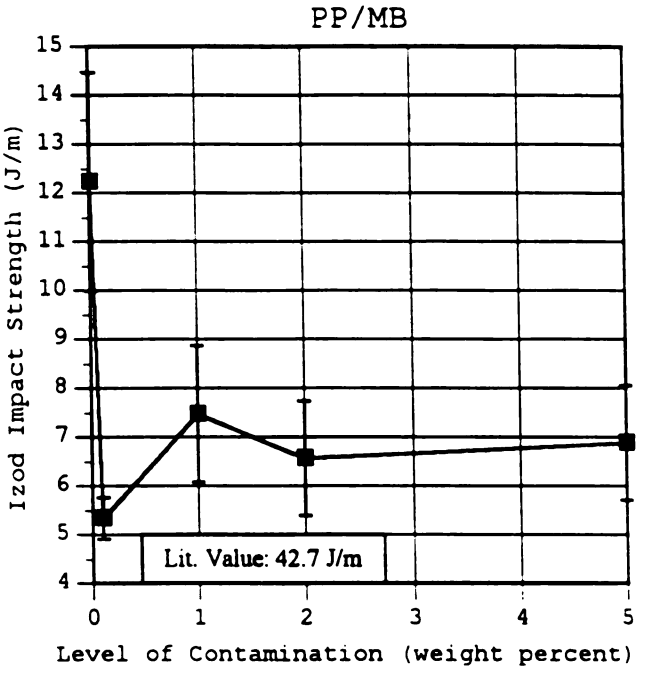

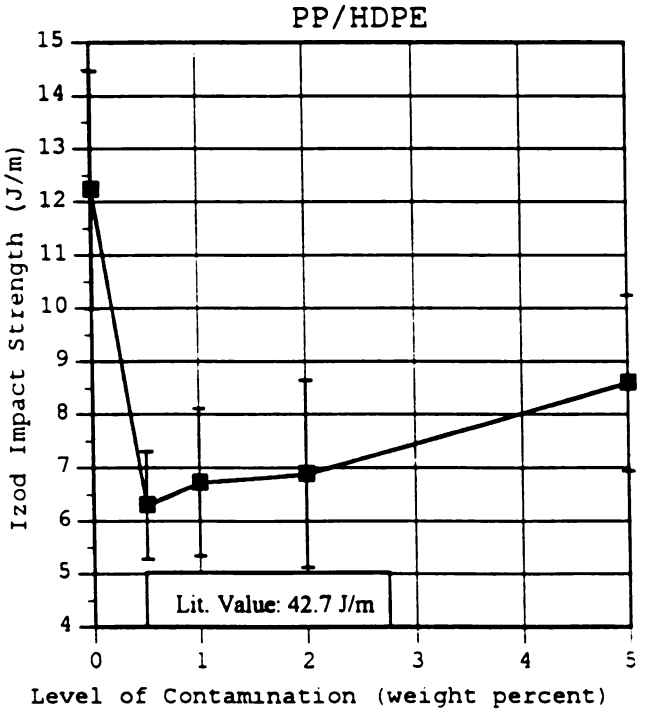

Figure 15: Effects of Contamination on Izod Impact Strength.

4.6.3 HDPE Contamination of PP - Although HDPE is often added to PP to improve PP impact resistance, very different results were observed in this study. A sharp decline in strength was seen at a contamination level of only .5 percent HDPE (Figure 15). At higher levels impact resistance did start to improve but at 5 percent contamination impact strength was still below that of the uncontaminated polymer.

4.7 Environmental Stress-Crack Resistance

4.7.1 Microbubble Contamination of HDPE - In order to find the 50 percent failure point, F_{50}, for each level of microbubble contamination, the failure time of each sample within the group was plotted against the percentage of samples that had failed up to that point (see Appendix). Logarithmic probability graph paper was used and the intersection of the best line fit with the 50 percent failure line gave the F_{50}.

A general decrease in ESCR was seen for the HDPE/MB samples (Figure 16) which was expected because of molded in stresses and a higher area of contact between the HDPE and the detergent.

4.7.2 PP Contamination of HDPE - PP contamination reduced the ESCR of HDPE (Figure 16). This is in contrast to the study by Christensen, *et al.* (13), in which PP improved HDPE's resistance to stress-cracking.

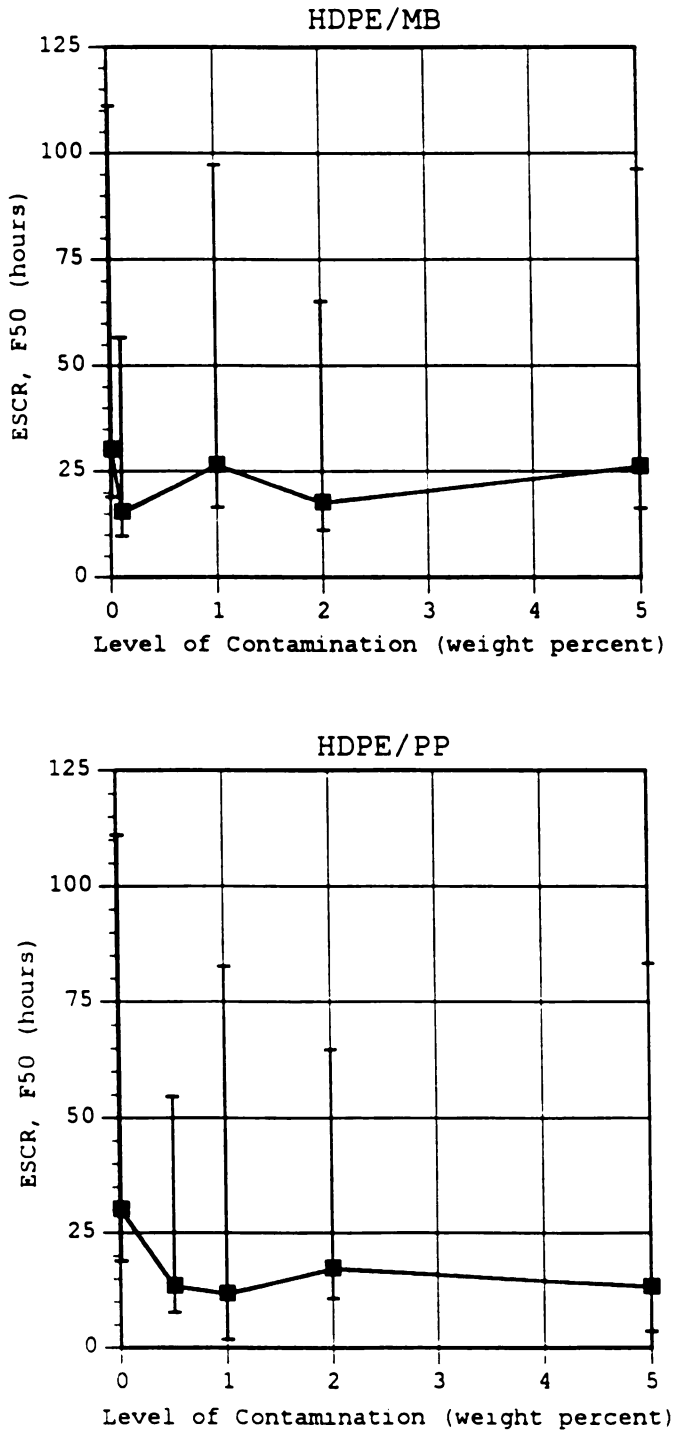

Figure 16: Effects of Contamination on Environmental Stress-Crack Resistance.

4.7.3 Contaminated PP - All of the PP samples tested either broke upon bending or did not break at all, up to 800 hours. No F_{50} can be reported for these groups, but it can be said that sufficient deterioration of PP was not imparted by the contamination to cause failure below 800 hours. Unrelated to the ESCR but worth mentioning is that failure upon bending increased with increased filler concentration (see Appendix B).

Flow Rate

4.8.1 Microbubble Contamination of the Polymer Matrices - Because the index length was not measured when determining HDPE flow rate, the flow rate cannot be converted to viscosity (see Appendix B), and no model can quantitatively predict the effect of a filler on HDPE flow rate. After an initial increase, the flow rate of HDPE declined as microbubble contamination increased (Figure 17). This decrease in flow rate is expected because of a disruption of the flow pattern and perhaps a hindrance to molecular orientation. The method of flow rate measurement used for PP allows the conversion to viscosity and a model for viscosity can thus be used to predict the effects of fillers on PP flow rate. PP flow rate was reduced with an increase of microbubble contamination, however, the effect is not as drastic as predicted by the Einstein model Figure 17).

4.8.2 HDPE/PP Cross-Contamination - The general effects seen on flow rates for the cross-contaminated polymers follows what would be expected intuitively. As the less viscous PP is added to HDPE more material flows through the capillary in a given time period (Figure 17). Increasing amounts of the viscous HDPE tend to decrease the flow rate of the polyblend melt.

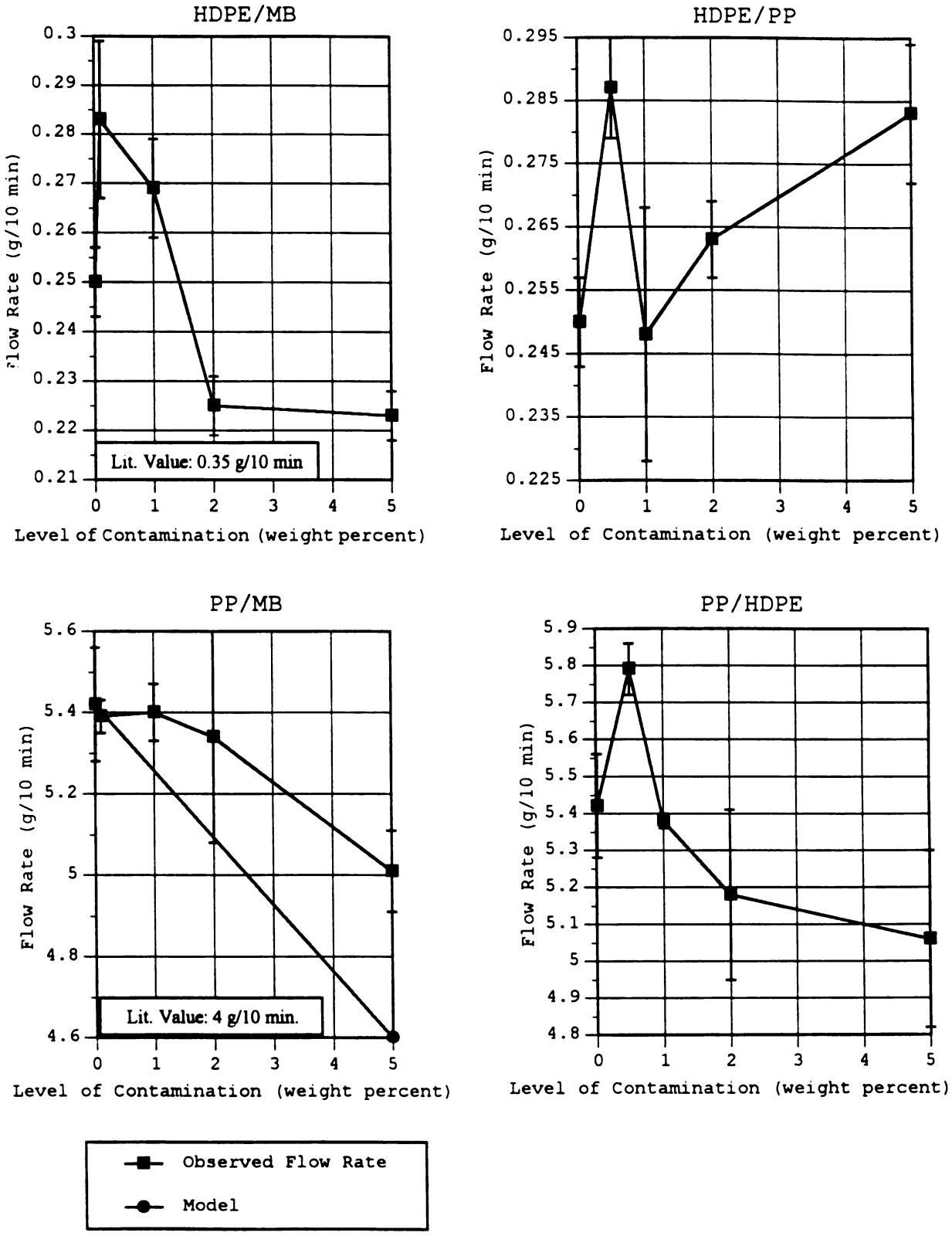

Figure 17: Effects of Contamination on Flow Rate.

CHAPTER V

SUMMARY AND CONCLUSIONS

In the processes used in this study, sample molding resulted in a high degree of microbubble breakage. This led to an increased density and may have decreased crystallinity in both polymer matrices. Polypropylene present in HDPE seemed to decrease the percent crystallinity of HDPE, while HDPE seemed to increase the percent crystallinity of PP. Many properties were slightly enhanced by various contamination levels (however, no added value is thought to accompany these increases), while most other properties tested stayed within typical ranges for the uncontaminated polymers. The main problem encountered for HDPE was a decrease in ESCR with the addition of either microbubbles or PP. This could result in bottle failure if closed-loop recycling is sought with products that accelerate environmental stress-cracking (such as oils and detergents). For PP the effect of contamination on impact strength is of greatest concern. The addition of 0.1 percent microbubbles or 0.5 percent HDPE (by weight) both result in a loss of impact strength of over 50 percent. This sharp initial effect at low levels of contamination is very characteristic of most of the properties studied.

The changes in flow rates caused by contamination were not drastic enough to render the polymer unprocessable, yet

there are several possible concerns. When changes in processing parameters are necessary, finding the optimum conditions can prove to be quite costly and time consuming. Also, the presence of the abrasive microbubbles could shorten the life of some of the processing equipment.

In an attempt to resolve the few problems encountered in this study, further experimentation is recommended in several areas. In order to improve the rheology of the polymer blends and thus the ultimate polymer properties, processing parameters along with appropriate compatibilizer use may be investigated. In an attempt to improve the ESCR of HDPE and the impact strength of PP with microbubble contamination, surface treatment of the glass may be considered.

Also, in view of implementing a cost effective and comprehensive curbside recycling program (concentrating still on the light fraction) several more separation processes must be investigated. This ambitious goal includes the separation of:

-Expanded polystyrene from the other light constituents present in common household waste (PP, HDPE, LDPE).

-Low density polyethylene from HDPE and PP.

-Blow molding grade PP from injection molding grade PP

-Blow molding grade HDPE from injection molding grade HDPE.

-Blow molding grade HDPE homopolymer from blow molding grade HDPE copolymer.

LIST OF REFERENCES

LIST OF REFERENCES

1. Vane, L.M., and Rodriguez, F., "Selective Dissolution: Multi-Solvent, Low Pressure Solution Process for Resource Recovery from Mixed Post-Consumer Platics," SPE RETEC, *Recy. Tech. of 1990's,* 100-106, Nov. 29-30, Chicago, IL.

2. "Key Markets Post Solid Gains in 1993," *Modern Plastics,* 73-81, January 1994.

3. Katz and Milewski, *Handbook of Fillers for Plastics,* Van Nostrand Reinhold Company, New York 1987.

4. Manson, J.A. and Sperling, L.H., *Polymer Blends and Composites,* Plenum Press, New York, 1976.

5. Nicolais, L. and Nicodemo, L., "Strength of Particulate Composites," *Polymer Engineering and Science,* Vol.13, No. 6, 469, November 1973.

6. Bigg, D.M., "Mechanical Properties of Particulate Filled Polymers," *Polymer Composites,* Vol. 8, No.2, 115-122, April 1987.

7. Levy, S. and Dubois, J.H., *Plastics Product Design Engineering Handbook,* Chapman and Hall, New York 1984.

8. Fraser, R., "Environmental Stress-Cracking of Plastics," *Plastics and Polymers,* 102-103, June 1975.

9. Sheldon, R.P., *Composite Polymeric Materials,* Applied Science Publishers, New York 1982.

10. Folks, M.J. and Hope, P.S., *Polymer Blends and Alloys,* Blackie Academic & Professional, New York 1993.

11. Paul, D.R. and Newman, S., *Polymer Blends,* Academic Press, New York 1978.

12. Harris, M.G., "The Physical Properties and Effects of Polymeric Contamination on Post-Consumer Recycled High Density Polyethylene," *Polyolefins VII RETEC*, 671-678, Houston, TX February 27,1991.

13. Christensen, R.E., Austin R.G., and Clayton D.M., "Polyolefin Blend Recycle Studies," SPE *ANTEC*, 794-798, Detroit, MI, May 3-7, 1992.

14. Lovinger, A.J. and Williams, M.L., "Tensile Properties and Morphology of Blends of Polyethylene and Polypropylene", *Journal of Applied Polymer Science*, Vol. 25, 1703-1713, 1980.

15. Kausch, H.H., *Polymer Fracture*, Sperling-Verlag, New York, 1978.

16. Kinney, *Enginnering Properties and Applications of Plastics*, John Wiley and Sons, Inc. New York 1957.

17. Lee, N.C., *Plastic Blow Molding Handbook*, Van Nostrand Reinhold, New York 1990.

18. Yang, D., Zhang, B., Yang, Y., Fang, Z., Sun, G., and Feng, Z., "Morphology and Properties of Blends of Polypropylene with Ethylene-Propylene Rubber", *Polymer Engineering and Science*, Vol. 24, No. 8, 612-617, June 1984.

APPENDIX A

Table 2: Effects of Contamination on Polymer Density.

(g/cm3)

HDPE Sample No.	Level of MB Contamination (wt %)				
	0	0.1	1	2	5
1	0.9493	0.9497	0.9526	0.9580	0.9643
2	0.9498	0.9493	0.9520	0.9577	0.9645
3	0.9495	0.9494	0.9512	0.9579	0.9609
Average	0.9495	0.9495	0.9519	0.9579	0.9632
St. Dev.	0.0003	0.0002	0.0007	0.0001	0.0020
HDPE Sample No.	Level of PP Contamination (wt %)				
	0	0.5	1	2	5
1	0.9493	0.9494	0.9491	0.9488	0.9453
2	0.9498	0.9479	0.9498	0.9473	0.9467
3	0.9495	0.9497	0.9492	0.9468	0.9462
Average	0.9496	0.9488	0.9495	0.9471	0.9464
St. Dev.	0.0002	0.0013	0.0004	0.0003	0.0003
PP Sample No.	Level of MB Contamination (wt %)				
	0	0.1	1	2	5
1	0.9070	0.9069	0.9102	0.9154	0.9214
2	0.9063	0.9068	0.9108	0.9139	0.9219
3	0.9061	0.9065	0.9104	0.9145	0.9216
Average	0.9064	0.9067	0.9105	0.9146	0.9216
St. Dev.	0.0005	0.0002	0.0003	0.0007	0.0002
PP Sample No.	Level of HDPE Contamination (wt %)				
	0	0.5	1	2	5
1	0.9070	0.9057	0.9065	0.9066	0.9074
2	0.9063	0.9057	0.9061	0.9062	0.9072
3	0.9061	0.9058	0.9058	0.9064	0.9077
Average	0.9064	0.9057	0.9061	0.9064	0.9074
St. Dev.	0.0005	0.0001	0.0004	0.0002	0.0002

Table 3: Effects of Contamination on Heat of Melting.

(J/g)

HDPE Sample No.	Level of MB Contamination (wt %) 0	0.1	1	2	5
1	198.8	185.9	178.7	179.2	180.0
2	192.7	193.4	183.8	193.0	185.0
Average	195.8	189.7	181.3	186.1	182.5
St. Dev.	4.3	5.3	3.6	9.8	3.5
HDPE Sample No.	Level of PP Contamination (wt %) 0	0.5	1	2	5
1	198.8	188.4	188.4	182.8	182.4
2	192.7	181.3	199.6	185.9	185.5
Average	195.8	184.9	194.0	184.4	183.9
St. Dev.	4.3	5.0	7.9	2.2	2.2
PP Sample No.	Level of MB Contamination (wt %) 0	0.1	1	2	5
1	86.73	86.79	86.26	91.42	79.28
2	96.11	94.64	-----	0.91	90.71
Average	91.42	90.72	86.26	46.17	85.00
St. Dev.	6.63	5.55	-----	64.00	8.08
PP Sample No.	Level of HDPE Contamination (wt %) 0	0.5	1	2	5
1	86.73	85.46	95.30	85.45	96.47
2	96.11	98.80	94.93	96.49	101.1
Average	91.42	92.13	95.12	90.97	98.79
St. Dev.	6.63	9.43	0.26	7.81	3.27

Table 4: Effects of Contamination on Tensile Strength at Yield.

(PSI)

HDPE Sample No.	Level of MB Contamination (wt %) 0	0.1	1	2	5
1	3620	3626	3624	3661	3864
2	3642	3691	3654	3714	3872
3	3615	3709	3702	3651	3920
4	3652	3757	3679	3709	3897
5	3645	3742	3693	3686	3872
6	3650	-----	-----	-----	-----
Average	3637	3705	3670	3684	3885
St. Dev.	16	51	32	28	23
HDPE Sample No.	Level of PP Contamination (wt %) 0	0.5	1	2	5
1	3620	3581	3719	3601	3590
2	3642	3772	3661	3626	3677
3	3615	3714	3722	3621	3680
4	3652	3767	3689	3634	3642
5	3645	3797	3757	3631	3645
6	3650	-----	-----	-----	-----
Average	3637	3726	3710	3623	3647
St. Dev.	16	87	36	13	36
PP Sample No.	Level of MB Contamination (wt %) 0	0.1	1	2	5
1	4402	4269	4204	4292	4327
2	4424	4382	4387	4334	4314
3	4392	4497	4322	4372	4445
4	4397	4412	4422	4357	4537
5	4384	4424	4349	4357	4314
Average	4400	4397	4337	4342	4387
St. Dev.	15	83	83	31	100
PP Sample No.	Level of HDPE Contamination (wt %) 0	0.5	1	2	5
1	4402	4550	4665	4617	4457
2	4424	4710	4673	4678	4547
3	4392	4610	4567	4630	4495
4	4397	4638	4567	4703	4600
5	4384	4648	4735	4622	4592
Average	4400	4631	4641	4650	4538
St. Dev.	15	58	73	38	62

Table 5: Effects of Contamination on Elongation at Yield.

(Percent)

HDPE Sample No.	Level of MB Contamination (wt %) 0	0.1	1	2	5
1	13.942	16.620	13.940	13.130	10.841
2	12.852	13.512	12.990	12.399	10.641
3	13.273	13.353	13.272	12.675	10.770
4	12.713	12.517	12.802	12.526	11.322
5	12.595	11.385	13.296	12.890	11.294
6	12.939	-----	-----	-----	-----
Average	13.052	13.477	13.260	12.724	10.974
St. Dev.	0.493	1.949	0.432	0.291	0.314
HDPE Sample No.	Level of PP Contamination (wt %) 0	0.5	1	2	5
1	13.942	15.890	12.102	16.281	13.953
2	12.852	13.936	12.737	14.778	12.379
3	13.273	14.551	11.935	12.960	14.148
4	12.713	12.821	12.805	13.221	12.730
5	12.595	13.505	13.289	12.762	13.797
6	12.939	-----	-----	-----	-----
Average	13.052	14.141	12.574	14.000	13.401
St. Dev.	0.493	1.164	0.553	1.502	0.793
PP Sample No.	Level of MB Contamination (wt %) 0	0.1	1	2	5
1	10.131	9.351	10.947	8.789	7.135
2	8.915	9.536	8.819	8.409	7.366
3	8.692	9.144	9.641	9.166	7.913
4	9.255	9.001	8.942	8.326	8.304
5	9.693	10.056	9.578	8.744	8.313
Average	9.337	9.418	9.585	8.687	7.806
St. Dev.	0.583	0.411	0.845	0.336	0.539
PP Sample No.	Level of HDPE Contamination (wt %) 0	0.5	1	2	5
1	10.131	10.767	10.774	9.757	10.071
2	8.915	10.036	10.295	9.217	9.553
3	8.692	10.016	10.227	9.400	10.347
4	9.255	10.382	10.693	9.255	9.961
5	9.693	9.942	10.479	9.390	9.256
Average	9.337	10.229	10.494	9.404	9.838
St. Dev.	0.583	0.346	0.239	0.213	0.433

Table 6: Effects of Contamination on Tensile Modulus of Elasticity.

(PSI)

HDPE Sample No.	Level of MB Contamination (wt %) 0	0.1	1	2	5
1	126300	128805	128377	154254	190610
2	128741	132262	155853	156749	160186
3	129658	165780	124209	156983	167270
4	129548	140788	130736	168730	170438
5	121795	137287	132302	161061	160127
Average	127208	140984	134295	159555	169726
St. Dev.	3315	14603	12431	5680	12508
HDPE Sample No.	Level of PP Contamination (wt %) 0	0.5	1	2	5
1	126300	119218	126723	113750	135571
2	128741	137211	136015	124909	135921
3	129658	133022	143846	116326	149369
4	129548	153692	135666	130526	128406
5	121795	149216	156164	129592	115690
Average	127208	138472	139683	123021	132991
St. Dev.	3315	13685	11028	7646	12286
PP Sample No.	Level of MB Contamination (wt %) 0	0.1	1	2	5
1	222751	192243	185311	141531	246689
2	192692	198597	220084	189219	220783
3	190267	178576	201602	175083	223781
4	200688	206632	181524	187756	225101
5	196106	184160	196920	171622	254556
Average	200501	192042	197088	173042	234182
St. Dev.	13040	11173	15249	19218	15344
PP Sample No.	Level of HDPE Contamination (wt %) 0	0.5	1	2	5
1	222751	203469	211847	297700	261116
2	192692	207063	218253	304502	330880
3	190267	187999	199899	310483	241640
4	200688	192989	202255	314810	254727
5	196106	218357	198121	298641	234191
Average	200501	201975	206075	305227	264511
St. Dev.	13040	11964	8626	7416	38583

Table 7: Effects of Contamination on Flexural Strength at 5% Strain.

(PSI)

HDPE Sample No.	Level of MB Contamination (wt %) 0	0.1	1	2	5
1	3352	3636	3567	3652	3849
2	3402	3522	3638	3641	3863
3	3359	3518	3586	3667	3856
4	3348	3494	3558	3638	3874
5	3329	3525	3570	3626	3891
Average	3358	3539	3584	3645	3867
St. Dev.	27	56	32	15	16
HDPE Sample No.	Level of PP Contamination (wt %) 0	0.5	1	2	5
1	3352	3530	3584	3480	3537
2	3402	3522	3501	3461	3548
3	3359	3603	3622	3473	3534
4	3348	3558	3650	3445	3518
5	3329	3556	3449	3452	3546
Average	3358	3554	3561	3462	3537
St. Dev.	27	32	84	14	12
PP Sample No.	Level of MB Contamination (wt %) 0	0.1	1	2	5
1	6601	6193	6417	6443	6722
2	6270	6181	6308	6534	6373
3	6313	6174	6534	6342	6782
4		6176	6306	6376	6407
5		6549	6246	6299	6448
Average	6395	6255	6362	6399	6546
St. Dev.	180	165	114	92	191
PP Sample No.	Level of HDPE Contamination (wt %) 0	0.5	1	2	5
1	6601	6450	6277	6157	6061
2	6270	7079	6123	6210	6368
3	6313	6507	6270	6325	6251
4	-----	6496	6248	6140	6094
5	-----	6279	6267	6159	6304
Average	6395	6562	6237	6198	6216
St. Dev.	180	303	65	76	133

Table 8: Effects of Contamination on Flexural Modulus of Elasticity.

(PSI)

HDPE Sample No.	Level of MB Contamination (wt %) 0	0.1	1	2	5
1	127900	138700	140600	133400	142000
2	128000	134500	140500	138100	141600
3	126300	136700	128700	140100	141200
4	127700	134500	138400	141000	141800
5	126400	134000	135600	136000	148200
Average	127260	135680	136760	137720	142960
St. Dev.	838	1985	4943	3090	2944
HDPE Sample No.	Level of PP Contamination (wt %) 0	0.5	1	2	5
1	127900	146700	137200	139300	130800
2	128000	138800	146200	139900	146500
3	126300	136800	137400	137700	145700
4	127700	136100	139200	132200	144500
5	126400	132600	137100	135800	133500
Average	127260	138200	139420	136980	140200
St. Dev.	838	5252	3886	3109	7444
PP Sample No.	Level of MB Contamination (wt %) 0	0.1	1	2	5
1	214200	208100	221400	227600	247000
2	209100	209200	217700	232200	233800
3	216800	210000	231600	223500	253300
4	-----	211100	220000	224500	232600
5	-----	226000	216600	221500	237500
Average	213367	212880	221460	225860	240840
St. Dev.	3917	7416	5973	4173	8970
PP Sample No.	Level of HDPE Contamination (wt %) 0	0.5	1	2	5
1	214200	225300	207200	205600	208100
2	209100	249800	204700	209600	219500
3	216800	229000	210600	215100	216100
4	-----	221300	209800	208100	208300
5	-----	212000	211400	207400	218200
Average	213367	227480	208740	209160	214040
St. Dev.	3917	13992	2755	3618	5468

Table 9: Effects of Contamination on Izod Impact Strength.

Impact Strength (FT.LB./IN.) and Type of Break
(c=Complete Break, h=Hinge Break)

	PP Sample No.	Level of MB Contamination (wt %) 0	0.1	1	2	5
	1	0.243 c	0.093 c	0.117 h	0.118 c	0.151 c
	2	0.244 c	0.104 c	0.106 c	0.104 c	0.122 c
	3	0.288 c	0.093 c	0.187 c	0.185 c	0.166 c
	4	0.202 c	0.105 c	0.163 c	0.116 c	0.119 c
	5	0.23 c	0.105 c	0.128 c	0.127 c	0.117 c
	6	0.256 c	0.092 c	0.117 c	0.104 h	0.107 c
	7	0.231 c	0.092 c	0.115 h	0.128 c	0.129 c
	8	0.117 h	0.104 c	0.128 c	0.127 c	0.119 c
	9	0.224 c	0.115 c	0.162 c	0.105 c	0.119 c
	10	0.236 c	0.093 c	0.163 c	0.116 c	0.108 c
	11	0.21 c	0.105 c	0.152 c	0.116 c	0.167 c
	12	0.253 c	-----	-----	0.127 c	-----
Total	Average	0.229	0.100	0.140	0.123	0.129
	St. Dev.	0.042	0.008	0.026	0.022	0.022
Hinge	Average	0.117	-----	0.116	0.104	-----
	St. Dev.	-----	-----	0.001	-----	-----
Complete	Average	0.239	0.100	0.145	0.124	0.129
	St. Dev.	0.024	0.008	0.027	0.022	0.022
	PP Sample No.	Level of HDPE Contamination (wt %) 0	0.5	1	2	5
	1	0.243 c	0.127 c	0.173 c	0.162 c	0.197 c
	2	0.244 c	0.139 c	0.139 c	0.184 c	0.163 c
	3	0.288 c	0.115 c	0.152 c	0.127 c	0.128 c
	4	0.202 c	0.115 c	0.149c	0.151 c	0.14 c
	5	0.23 c	0.103 c	0.103 h	0.15 c	0.153 c
	6	0.265 c	0.107 c	0.126 c	0.115 c	0.163 c
	7	0.231 c	0.105 c	0.093 c	0.104 h	0.162 c
	8	0.117 h	0.116 c	0.105 c	0.126 c	0.138 c
	9	0.224 c	0.094 c	0.139 c	0.058 h	0.221 c
	10	0.236 c	0.164 c	0.093 h	0.116 h	0.188 c
	11	0.21 c	0.115 c	0.116 h	0.127 c	0.116 c
	12	0.253 c	-----	-----	-----	-----
Total	Average	0.229	0.118	0.126	0.129	0.161
	St. Dev.	0.042	0.019	0.026	0.033	0.031
Hinge	Average	0.117	-----	0.104	0.093	-----
	St. Dev.	-----	-----	0.012	0.031	-----
Complete	Average	0.239	0.118	0.135	0.143	0.161
	St. Dev.	0.024	0.019	0.026	0.023	0.031

Table 10: Effects of Contamination on Environmental Stress-Crack Resistance.

Hours to Failure

HDPE Sample No.	Level of MB Contamination (wt %) 0	0.1	1	2	5
1	8	6	11	11	12
2	17	12	13	11	17
3	18	13	15	13	27
4	20	13	23	14	27
5	22	13	25	17	27
6	24	14	26	18	27
7	50	16	32	19	27
8	80	17	33	26	29
9	80	21	80	27	34
10	80	80	80	30	38
F50	30.0	15.3	26.3	17.6	26.0
HDPE Sample No.	Level of PP Contamination (wt %) 0	0.5	1	2	5
1	8	6	4	5	4
2	17	8	10	14	9
3	18	8	10	15	11
4	20	8	10	16	11
5	22	11	10	16	12
6	24	12	13	19	15
7	50	17	13	25	17
8	80	20	15	26	18
9	80	38	16	29	29
10	80	42	26	30	30
F50	30.0	13.3	11.6	17.2	13.2

Table 11: Effects of Contamination on Flow Rate.

(g/10 min)

HDPE Sample No.	Level of MB Contamination (wt %) 0	0.1	1	2	5
1	0.257	0.279	0.281	0.224	0.229
2	0.249	0.271	0.267	0.232	0.220
3	0.244	0.301	0.261	0.220	0.220
Average	0.250	0.284	0.270	0.225	0.223
St. Dev.	0.007	0.016	0.010	0.006	0.005
HDPE Sample No.	Level of PP Contamination (wt %) 0	0.5	1	2	5
1	0.257	0.279	0.235	0.269	0.274
2	0.249	0.286	0.237	0.264	0.281
3	0.244	0.296	0.271	0.257	0.296
Average	0.250	0.287	0.248	0.263	0.284
St. Dev.	0.007	0.009	0.020	0.006	0.011
PP Sample No.	Level of MB Contamination (wt %) 0	0.1	1	2	5
1	5.31	5.38	5.32	5.05	5.00
2	5.57	5.43	5.46	5.56	5.12
3	5.38	5.36	5.41	5.42	4.91
Average	5.42	5.39	5.40	5.34	5.01
St. Dev.	0.13	0.04	0.07	0.26	0.11
PP Sample No.	Level of HDPE Contamination (wt %) 0	0.5	1	2	5
1	5.31	5.85	5.39	4.93	4.80
2	5.57	5.71	5.35	5.35	5.10
3	5.38	5.81	5.39	5.28	5.28
Average	5.42	5.79	5.38	5.19	5.06
St. Dev.	0.13	0.07	0.02	0.23	0.24

APPENDIX B

Table 12: Calculated Microbubble Breakage in HDPE and PP.

HDPE/MB	Level of Glass Microbubbles Added (wt %)				
	0	0.1	1	2	5
Density of Resin	0.9495	0.9495	0.9519	0.9579	0.9632
Volume Fraction Intact Bubbles	0.0000	0.000691	0.004049	0.003819	0.017333
Volume Fraction Broken Bubbles	0.0000	0.000308	0.003349	0.007116	0.016544
Percentage of Bubbles Broken	----------	81.05	88.83	94.71	90.17
Total Volume Load Glass	0.0000	0.000999	0.007398	0.010934	0.033877

Average Percentage of Microbubble Breakage in HDPE **88.69**

PP/MB	Level of Glass Microbubble Added (wt %)				
	0	0.1	1	2	5
Density of Resin	0.9064	0.9067	0.9105	0.9146	0.9216
Volume Fraction Intact Bubbles	0.0000	0.000341	0.002027	0.003979	0.015729
Volume Fraction Broken Bubbles	0.0000	0.000327	0.003395	0.00676	0.015918
Percentage of Bubbles Broken	----------	90.21	94.15	94.23	90.68
Total Volume Load Glass	0.0000	0.000668	0.005422	0.010738	0.031647

Average Percentage of Microbubble Breakage in PP **92.32**

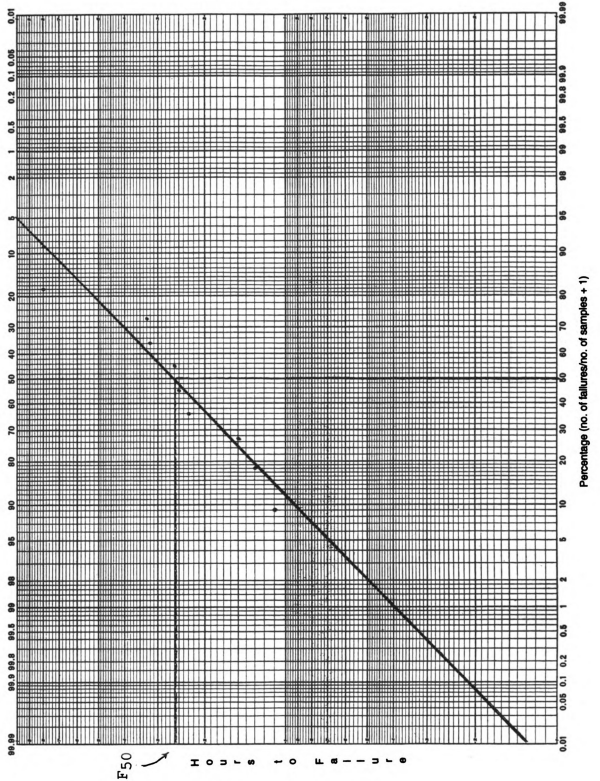

Figure 19: Graphical Method Used to Determine Environmental Stress-Crack Resistance

Figure 13: Number of PP Samples to Break Upon Bending When Testing for Environmental Stress-Crack Resistance.

Level of MB Contamination	0	0.1	1	2	5
No. of Failures Upon Bending	1	6	6	1	8

Level of PP Contamination	0	0.5	1	2	5
No. of Failures Upon Bending	1	1	1	3	3

$$\text{Viscosity} = \frac{\text{Shear Stress}}{\text{Shear Rate}}$$

$$\text{Shear Stress} = \frac{Fr}{2^{\pi R^2 L}}$$

$$\text{Shear Rate} = \frac{4\pi R^2 L_1}{\pi r^3 T}$$

where, F = Load on ram, kg
r = Orifice radius, mm
R = Barrel radius, mm
L = Orifice length, mm
L_1= Index length, mm
T = Index extrusion time, sec.

Figure 19: Equations Used to Convert Flow Rate to Viscosity.

APPENDIX C

APPENDIX C

Analysis of Variance

Anova: Density - HDPE/MB							
Summary							
Groups	*Count*	*Sum*	*Average*	*Variance*			
Pure HDPE	3	2.848552	0.949517	6.29E-08			
HDPE/.1%MB	3	2.848409	0.94947	5.56E-08			
HDPE/1%MB	3	2.855837	0.951946	4.99E-07			
HDPE/2%MB	3	2.873616	0.957872	1.65E-08			
HDPE/5%MB	3	2.889679	0.963226	4.05E-06			
ANOVA							
Source of Variation							
		SS	*df*	*MS*	*F*	*P-value*	*F crit*
Between Groups		0.000432	4	0.000108	115.3218	2.53E-08	3.47805
Within Groups		9.37E-06	10	9.37E-07			
Total		0.000442	14				

Anova: Density - HDPE/PP							
Summary							
Groups	*Count*	*Sum*	*Average*	*Variance*			
Pure HDPE	3	2.848552	0.949517	6.29E-08			
HDPE/.5%PP	3	2.846998	0.948999	9.51E-07			
HDPE/1%PP	3	2.848124	0.949375	1.41E-07			
HDPE/2%PP	3	2.842985	0.947662	1.11E-06			
HDPE/5%PP	3	2.838158	0.946053	4.96E-07			
ANOVA							
Source of Variation							
		SS	*df*	*MS*	*F*	*P-value*	*F crit*
Between Groups		2.57E-05	4	6.44E-06	11.65937	0.000878	3.47805
Within Groups		5.52E-06	10	5.52E-07			
Total		3.13E-05	14				

Anova: Density - PP/MB							
Summary							
Groups	*Count*	*Sum*	*Average*	*Variance*			
Pure PP	3	2.719345	0.906448	2.48E-07			
PP/.1%MB	3	2.720183	0.906728	3.63E-08			
PP/%MB	3	2.731359	0.910453	8.46E-08			
PP/2%MB	3	2.743789	0.914596	5E-07			
PP/5%MB	3	2.764944	0.921648	5.29E-08			
ANOVA							
Source of Variation							
		SS	*df*	*MS*	*F*	*P-value*	*F crit*
Between Groups		0.000483	4	0.000121	654.7633	4.76E-12	3.47805
Within Groups		1.84E-06	10	1.84E-07			
Total		0.000484	14				

Anova: Density for PP/HDPE							
Summary							
Groups	*Count*	*Sum*	*Average*	*Variance*			
Pure PP	3	2.719345	0.906448	2.48E-07			
PP/.5%HDPE	3	2.717153	0.905718	3.5E-09			
PP/%HDPE	3	2.718342	0.906114	1.41E-07			
PP/2%HDPE	3	2.719199	0.9064	3.26E-08			
PP/5%HDPE	3	2.722335	0.907445	4.16E-08			
ANOVA							
Source of Variation							
		SS	*df*	*MS*	*F*	*P-value*	*F crit*
Between Groups		4.92E-06	4	1.23E-06	13.17115	0.000538	3.47805
Within Groups		9.33E-07	10	9.33E-08			
Total		5.85E-06	14				

Anova: Tensile Strength at Yield - HDPE/MB							
Summary							
Groups	*Count*	*Sum*	*Average*	*Variance*			
Pure HDPE	6	21824	3637.333	251.0667			
HDPE/.1%MB	5	18525	3705	2631.5			
HDPE/1%MB	5	18352	3670.4	1001.3			
HDPE/2%MB	5	18421	3684.2	786.7			
HDPE/5%MB	5	19425	3885	537			
ANOVA							
Source of Variation							
		SS	*df*	*MS*	*F*	*P-value*	*F crit*
Between Groups		195810.6	4	48952.64	48.76377	2.46E-10	2.840096
Within Groups		21081.33	21	1003.873			
Total		216891.9	25				

Anova: Tensile Strength at Yield - HDPE/PP							
Summary							
Groups	*Count*	*Sum*	*Average*	*Variance*			
Pure HDPE	6	21824	3637.333	251.0667			
HDPE/.5%PP	5	18631	3726.2	7501.7			
HDPE/1%PP	5	18548	3709.6	1318.8			
HDPE/2%PP	5	18113	3622.6	170.3			
HDPE/5%PP	5	18234	3646.8	1316.7			
ANOVA							
Source of Variation							
		SS	*df*	*MS*	*F*	*P-value*	*F crit*
Between Groups		43772.21	4	10943.05	5.409021	0.003732	2.840096
Within Groups		42485.33	21	2023.111			
Total		86257.54	25				

Anova: Tensile Strength at Yield - PP/MB							
Summary							
Groups	*Count*	*Sum*	*Average*	*Variance*			
Pure PP	5	21999	4399.8	227.2			
PP/.1%MB	5	21984	4396.8	6890.7			
PP/%MB	5	21684	4336.8	6945.7			
PP/2%MB	5	21712	4342.4	978.3			
PP/5%MB	5	21937	4387.4	10030.3			
ANOVA							
Source of Variation							
		SS	*df*	*MS*	*F*	*P-value*	*F crit*
Between Groups		18690.96	4	4672.74	0.931857	0.465463	2.866081
Within Groups		100288.8	20	5014.44			
Total		118979.8	24				

Anova: Tensile Strength at Yield - PP/HDPE							
Summary							
Groups	*Count*	*Sum*	*Average*	*Variance*			
Pure PP	5	21999	4399.8	227.2			
PP/.5%HDPE	5	23156	4631.2	3395.2			
PP/%HDPE	5	23207	4641.4	5346.8			
PP/2%HDPE	5	23250	4650	1466.5			
PP/5%HDPE	5	22691	4538.2	3812.7			
ANOVA							
Source of Variation							
		SS	*df*	*MS*	*F*	*P-value*	*F crit*
Between Groups		226001	4	56500.26	19.82688	9.86E-07	2.866081
Within Groups		56993.6	20	2849.68			
Total		282994.6	24				

Anova: Elongation at Yield - HDPE/MB							
Summary							
Groups	*Count*	*Sum*	*Average*	*Variance*			
Pure HDPE	6	78.314	13.05233	0.243496			
HDPE/.1%MB	5	67.387	13.4774	3.798278			
HDPE/1%MB	5	66.3	13.26	0.186626			
HDPE/2%MB	5	63.62	12.724	0.084905			
HDPE/5%MB	5	54.868	10.9736	0.098424			
ANOVA							
Source of Variation							
		SS	*df*	*MS*	*F*	*P-value*	*F crit*
Between Groups		20.23654	4	5.059135	5.938477	0.00233	2.840096
Within Groups		17.89042	21	0.851925			
Total		38.12695	25				

Anova: Elongation at Yield - HDPE/PP							
Summary							
Groups	*Count*	*Sum*	*Average*	*Variance*			
Pure HDPE	6	78.314	13.05233	0.243496			
HDPE/.5%PP	5	70.703	14.1406	1.354005			
HDPE/1%PP	5	62.868	12.5736	0.305565			
HDPE/2%PP	5	70.002	14.0004	2.257332			
HDPE/5%PP	5	67.007	13.4014	0.628563			
ANOVA							
Source of Variation							
		SS	*df*	*MS*	*F*	*P-value*	*F crit*
Between Groups		8.675384	4	2.168846	2.347799	0.087556	2.840096
Within Groups		19.39934	21	0.923778			
Total		28.07473	25				

Anova: Elongation at Yield - PP/MB							
Summary							
Groups	*Count*	*Sum*	*Average*	*Variance*			
Pure PP	5	46.686	9.3372	0.339501			
PP/.1%MB	5	47.088	9.4176	0.168605			
PP/%MB	5	47.927	9.5854	0.714608			
PP/2%MB	5	43.434	8.6868	0.112675			
PP/5%MB	5	39.031	7.8062	0.290086			
ANOVA							
Source of Variation							
		SS	*df*	*MS*	*F*	*P-value*	*F crit*
Between Groups		10.74237	4	2.685594	8.26095	0.00042	2.866081
Within Groups		6.501901	20	0.325095			
Total		17.24428	24				

Anova: Elongation at Yield - PP/HDPE							
Summary							
Groups	*Count*	*Sum*	*Average*	*Variance*			
Pure PP	5	46.686	9.3372	0.339501			
PP/.5%HDPE	5	51.143	10.2286	0.11946			
PP/%HDPE	5	52.468	10.4936	0.057279			
PP/2%HDPE	5	47.019	9.4038	0.045498			
PP/5%HDPE	5	49.188	9.8376	0.187112			
ANOVA							
Source of Variation							
		SS	*df*	*MS*	*F*	*P-value*	*F crit*
Between Groups		5.096274	4	1.274069	8.506842	0.000353	2.866081
Within Groups		2.995397	20	0.14977			
Total		8.091671	24				

Anova: Tensile Modulus of Elasticity - HDPE/MB							
Summary							
Groups	*Count*	*Sum*	*Average*	*Variance*			
Pure HDPE	5	636042	127208.4	10988305			
HDPE/.1%MB	5	704922	140984.4	2.13E+08			
HDPE/1%MB	5	671477	134295.4	1.55E+08			
HDPE/2%MB	5	797777	159555.4	32259520			
HDPE/5%MB	5	848631	169726.2	1.56E+08			
ANOVA							
Source of Variation							
		SS	*df*	*MS*	*F*	*P-value*	*F crit*
Between Groups		6.31E+09	4	1.58E+09	13.89189	1.41E-05	2.866081
Within Groups		2.27E+09	20	1.13E+08			
Total		8.58E+09	24				

Anova: Tensile Modulus of Elasticity - HDPE/PP							
Summary							
Groups	*Count*	*Sum*	*Average*	*Variance*			
Pure HDPE	5	636042	127208.4	10988305			
HDPE/.5%PP	5	692359	138471.8	1.87E+08			
HDPE/1%PP	5	698414	139682.8	1.22E+08			
HDPE/2%PP	5	615103	123020.6	58460519			
HDPE/5%PP	5	664957	132991.4	1.51E+08			
ANOVA							
Source of Variation							
		SS	*df*	*MS*	*F*	*P-value*	*F crit*
Between Groups		1.03E+09	4	2.56E+08	2.421849	0.082093	2.866081
Within Groups		2.12E+09	20	1.06E+08			
Total		3.14E+09	24				

Anova: Tensile Modulus of Elasticity - PP/MB							
Summary							
Groups	*Count*	*Sum*	*Average*	*Variance*			
Pure PP	5	1002504	200500.8	1.7E+08			
PP/.1%MB	5	960208	192041.6	1.25E+08			
PP/%MB	5	985441	197088.2	2.33E+08			
PP/2%MB	5	865211	173042.2	3.69E+08			
PP/5%MB	5	1170910	234182	2.35E+08			
ANOVA							
Source of Variation							
		SS	*df*	*MS*	*F*	*P-value*	*F crit*
Between Groups		9.83E+09	4	2.46E+09	10.84882	7.66E-05	2.866081
Within Groups		4.53E+09	20	2.26E+08			
Total		1.44E+10	24				

Anova: Tensile Modulus of Elasticity - PP/HDPE							
Summary							
Groups	*Count*	*Sum*	*Average*	*Variance*			
Pure PP	5	1002504	200500.8	1.7E+08			
PP/.5%HDPE	5	1009877	201975.4	1.43E+08			
PP/%HDPE	5	1030375	206075	74405290			
PP/2%HDPE	5	1526136	305227.2	55004044			
PP/5%HDPE	5	1322554	264510.8	1.49E+09			
ANOVA							
Source of Variation							
		SS	*df*	*MS*	*F*	*P-value*	*F crit*
Between Groups		4.46E+10	4	1.11E+10	28.86172	4.69E-08	2.866081
Within Groups		7.72E+09	20	3.86E+08			
Total		5.23E+10	24				

Anova: Flexural Strength at 5% Strain - HDPE/MB							
Summary							
Groups	*Count*	*Sum*	*Average*	*Variance*			
Pure HDPE	5	16790	3358	728.5			
HDPE/.1%MB	5	17695	3539	3090			
HDPE/1%MB	5	17919	3583.8	1020.2			
HDPE/2%MB	5	18224	3644.8	239.7			
HDPE/5%MB	5	19333	3866.6	271.3			
ANOVA							
Source of Variation							
		SS	*df*	*MS*	*F*	*P-value*	*F crit*
Between Groups		678089.4	4	169522.3	158.441	7.68E-15	2.866081
Within Groups		21398.8	20	1069.94			
Total		699488.2	24				

Anova: Flexural Strength at 5% Strain - HDPE/PP							
Summary							
Groups	*Count*	*Sum*	*Average*	*Variance*			
Pure HDPE	5	16790	3358	728.5			
HDPE/.5%PP	5	17769	3553.8	1005.2			
HDPE/1%PP	5	17806	3561.2	7078.7			
HDPE/2%PP	5	17311	3462.2	208.7			
HDPE/5%PP	5	17683	3536.6	142.8			
ANOVA							
Source of Variation							
		SS	*df*	*MS*	*F*	*P-value*	*F crit*
Between Groups		147066.2	4	36766.54	20.06053	9E-07	2.866081
Within Groups		36655.6	20	1832.78			
Total		183721.8	24				

Anova: Flexural Strength at 5% Strain - PP/MB							
Summary							
Groups	*Count*	*Sum*	*Average*	*Variance*			
Pure PP	3	19184	6394.667	32392.33			
PP/.1%MB	5	31273	6254.6	27139.3			
PP/%MB	5	31811	6362.2	13029.2			
PP/2%MB	5	31994	6398.8	8484.7			
PP/5%MB	5	32732	6546.4	36381.3			
ANOVA							
Source of Variation							
		SS	*df*	*MS*	*F*	*P-value*	*F crit*
Between Groups		218262.3	4	54565.57	2.4256	0.085717	2.927749
Within Groups		404922.7	18	22495.7			
Total		623185	22				

Anova: Flexural Strength at 5% Strain - PP/HDPE							
Summary							
Groups	*Count*	*Sum*	*Average*	*Variance*			
Pure PP	3	19184	6394.667	32392.33			
PP/.5%HDPE	5	32811	6562.2	91825.7			
PP/%HDPE	5	31185	6237	4176.5			
PP/2%HDPE	5	30991	6198.2	5709.7			
PP/5%HDPE	5	31078	6215.6	17745.3			
ANOVA							
Source of Variation							
		SS	*df*	*MS*	*F*	*P-value*	*F crit*
Between Groups		472611.8	4	118153	3.919463	0.018471	2.927749
Within Groups		542613.5	18	30145.19			
Total		1015225	22				

Anova: Flexural Modulus of Elasticity - HDPE/MB							
Summary							
Groups	*Count*	*Sum*	*Average*	*Variance*			
Pure HDPE	5	636300	127260	703000			
HDPE/.1%MB	5	678400	135680	3942000			
HDPE/1%MB	5	683800	136760	24433000			
HDPE/2%MB	5	688600	137720	9547000			
HDPE/5%MB	5	714800	142960	8668000			
ANOVA							
Source of Variation							
		SS	*df*	*MS*	*F*	*P-value*	*F crit*
Between Groups		6.42E+08	4	1.61E+08	16.9738	3.25E-06	2.866081
Within Groups		1.89E+08	20	9458600			
Total		8.31E+08	24				

Anova: Flexural Modulus of Elasticity - HDPE/PP							
Summary							
Groups	*Count*	*Sum*	*Average*	*Variance*			
Pure HDPE	5	636300	127260	703000			
HDPE/.5%PP	5	691000	138200	27585000			
HDPE/1%PP	5	697100	139420	15102000			
HDPE/2%PP	5	684900	136980	9667000			
HDPE/5%PP	5	701000	140200	55420000			
ANOVA							
Source of Variation							
		SS	*df*	*MS*	*F*	*P-value*	*F crit*
Between Groups		5.53E+08	4	1.38E+08	6.376679	0.001776	2.866081
Within Groups		4.34E+08	20	21695400			
Total		9.87E+08	24				

Anova: Flexural Modulus of Elasticity - PP/MB							
Summary							
Groups	*Count*	*Sum*	*Average*	*Variance*			
Pure PP	3	640100	213366.7	15343333			
PP/.1%MB	5	1137400	227480	1.96E+08			
PP/%MB	5	1043700	208740	7588000			
PP/2%MB	5	1045800	209160	13093000			
PP/5%MB	5	1070200	214040	29898000			
ANOVA							
Source of Variation							
		SS	*df*	*MS*	*F*	*P-value*	*F crit*
Between Groups		1.16E+09	4	2.89E+08	5.116109	0.00623	2.927749
Within Groups		1.02E+09	18	56448370			
Total		2.17E+09	22				

Anova: Flexural Modulus of Elasticity - PP/HDPE							
Summary							
Groups	*Count*	*Sum*	*Average*	*Variance*			
Pure PP	3	640100	213366.7	15343333			
PP/.5%HDPE	5	1137400	227480	1.96E+08			
PP/%HDPE	5	1043700	208740	7588000			
PP/2%HDPE	5	1045800	209160	13093000			
PP/5%HDPE	5	1070200	214040	29898000			
ANOVA							
Source of Variation							
		SS	*df*	*MS*	*F*	*P-value*	*F crit*
Between Groups		1.16E+09	4	2.89E+08	5.116109	0.00623	2.927749
Within Groups		1.02E+09	18	56448370			
Total		2.17E+09	22				

Anova: Flow Rate - HDPE/MB							
Summary							
Groups	*Count*	*Sum*	*Average*	*Variance*			
Pure HDPE	3	0.75	0.25	4.3E-05			
HDPE/.1%MB	3	0.851	0.283667	0.000241			
HDPE/1%MB	3	0.809	0.269667	0.000105			
HDPE/2%MB	3	0.676	0.225333	3.73E-05			
HDPE/5%MB	3	0.669	0.223	2.7E-05			
ANOVA							
Source of Variation							
		SS	*df*	*MS*	*F*	*P-value*	*F crit*
Between Groups		0.008571	4	0.002143	23.59949	4.45E-05	3.47805
Within Groups		0.000908	10	9.08E-05			
Total		0.009479	14				

Anova: Flow Rate - HDPE/PP							
Summary							
Groups	*Count*	*Sum*	*Average*	*Variance*			
Pure HDPE	3	0.75	0.25	4.3E-05			
HDPE/.5%PP	3	0.861	0.287	7.3E-05			
HDPE/1%PP	3	0.743	0.247667	0.000409			
HDPE/2%PP	3	0.79	0.263333	3.63E-05			
HDPE/5%PP	3	0.851	0.283667	0.000126			
ANOVA							
Source of Variation							
		SS	*df*	*MS*	*F*	*P-value*	*F crit*
Between Groups		0.004055	4	0.001014	7.367975	0.00494	3.47805
Within Groups		0.001376	10	0.000138			
Total		0.005431	14				

Anova: Flow Rate - PP/MB							
Summary							
Groups	*Count*	*Sum*	*Average*	*Variance*			
Pure PP	3	16.26	5.42	0.0181			
PP/.1%MB	3	16.17	5.39	0.0013			
PP/%MB	3	16.19	5.396667	0.005033			
PP/2%MB	3	16.03	5.343333	0.069433			
PP/5%MB	3	15.03	5.01	0.0111			
ANOVA							
Source of Variation							
		SS	*df*	*MS*	*F*	*P-value*	*F crit*
Between Groups		0.351307	4	0.087827	4.18355	0.03024	3.47805
Within Groups		0.209933	10	0.020993			
Total		0.56124	14				

Anova: Flow Rate - PP/HDPE							
Summary							
Groups	*Count*	*Sum*	*Average*	*Variance*			
Pure PP	3	16.26	5.42	0.0181			
PP/.5%HDPE	3	17.37	5.79	0.0052			
PP/%HDPE	3	16.13	5.376667	0.000533			
PP/2%HDPE	3	15.56	5.186667	0.050633			
PP/5%HDPE	3	15.18	5.06	0.0588			
ANOVA							
Source of Variation							
		SS	*df*	*MS*	*F*	*P-value*	*F crit*
Between Groups		0.9258	4	0.23145	8.683717	0.002725	3.47805
Within Groups		0.266533	10	0.026653			
Total		1.192333	14				